Title: Separate neural representations of prediction error valence and surprise: evidence from an fMRI meta-analysis

Short title: Separate neural correlates of prediction error valence and surprise

Authors: Elsa Fouragnan[1,2], Chris Retzler[1,3] and Marios G. Philiastides[1]

Affiliations: [1]Institute of Neuroscience & Psychology, University of Glasgow, Glasgow, UK. [2]Department of Experimental Psychology, University of Oxford, Oxford, UK, [3]Department of Behavioural & Social Sciences, University of Huddersfield, Huddersfield, UK.

Acknowledgements: Funding for this work was provided by the Biotechnology and Biological Sciences Research Council (BBSRC; grants BB/J015393/1–2 to M.G.P.) and the Economic and Social Research Council (ESRC; grant ES/L012995/1 to M.G.P.). We also thank Dr. Andrea Pisauro, Dr. Miriam Klein-Flugge and Dr. Jacqueline Scholl for helpful comments on the manuscript.

Abstract

Learning occurs when an outcome differs from expectations, generating a reward prediction error signal (RPE). The RPE signal has been hypothesized to simultaneously embody the valence of an outcome (better or worse than expected) and its surprise (how far from expectations). Nonetheless, growing evidence suggests that separate representations of the two RPE components exist in the human brain. Meta-analyses provide an opportunity to test this hypothesis and directly probe the extent to which the valence and surprise of the error signal are encoded in *separate* or *overlapping* networks. We carried out several meta-analyses on a large set of fMRI studies investigating the neural basis of RPE, locked at decision outcome. We identified two valence learning systems by pooling studies searching for differential neural activity in response to *categorical* positive-vs-negative outcomes. The first valence network (negative > positive) involved areas regulating alertness and switching behaviors such as the midcingulate cortex, the thalamus and the dorsolateral prefrontal cortex whereas the second valence network (positive > negative) encompassed regions of the human reward circuitry such as the ventral striatum and the ventromedial prefrontal cortex. We also found evidence of a largely distinct surprise-encoding network including the anterior cingulate cortex, anterior insula and dorsal striatum. Together with recent animal and electrophysiological evidence this meta-analysis points to a sequential and distributed encoding of different components of the RPE signal, with potentially distinct functional roles.

Introduction

Effective decision-making depends upon accurate outcome representations associated with potential choices. These representations can be defined through reinforcement learning (RL) [Rescorla and Wagner, 1972; Sutton, 1998], a modelling framework that uses the reward prediction error (RPE), the difference between actual and expected outcomes, as a learning signal to update future outcome expectations. In this framework, RPE is a signed quantity and learning is driven by two separate components of the RPE signal: its *valence* (i.e. the sign of the RPE, representing whether an outcome is better [+] or worse [-] than expected) and its *surprise* (i.e. the modulus of the RPE, representing the degree [high or low] of deviation from expectations). Whereas the valence informs an agent whether to reinforce or extinguish a certain behaviour [Fouragnan et al., 2015; Fouragnan et al., 2017; Frank et al., 2004], the surprise component determines the extent to which the strength of association between outcome and expectations needs to be adjusted [Collins and Frank, 2016; Niv et al., 2015; den Ouden et al., 2012].

This modelling framework has received considerable attention in neuroscience since the early 90's when animal neurophysiological studies identified dopaminergic neurons in the midbrain, in particular in the ventral tegmental area (VTA), the substantia nigra pars compacta (SNc) and reticulata (SNr), whose tonic response profile appears to simultaneously capture both components of the RPE signal outlined above [Montague et al., 1996; Schultz et al., 1993; Schultz et al., 1997]. Specifically, these neurons show anticipatory increase and suppression of their tonic activity in response to positive and negative RPE respectively. While the anticipatory increase is proportional to the magnitude of positive RPE, the magnitude of negative RPE is encoded by the duration of the basal tonic suppression.

This discovery was a breakthrough in the field of learning and decision making and has continued to be influential in the field over the past two and half decades (see [Schultz, 2016a; Schultz, 2016b] for a review). As a result, this neurophysiological work has strongly motivated human functional magnetic resonance imaging (fMRI) research to identify the corresponding macroscopic Blood-Oxygen-Level-Dependent (BOLD) pattern of the signed RPE. This pattern of activity was expected to be such that the strength of the BOLD would proceed from high positive RPEs > low positive RPEs > low negative RPEs > high negative RPEs. More specifically, studies have employed a model-based fMRI approach, whereby different types of reinforcement-learning models are first fitted to subjects' behavior to yield parametric predictors for signed RPE against which fMRI data are subsequently regressed [Daw et al., 2011; Fouragnan et al., 2013; Gläscher et al., 2010; O'Doherty et al., 2004; O'doherty et al., 2007; Queirazza et al., 2017].

These fMRI studies have employed different algorithms to derive the signed RPE, ranging from the simple formulation of the temporal difference learning algorithm to incorporating action learning, notably using the Q-learning and SARSA ('state, action, reward, state, and action') algorithms [Schonberg et al., 2010; Seymour et al., 2007; Tanaka et al., 2006]. According to qualitative reviews of this previous findings [O'doherty et al., 2007] as well as quantitative, coordinate-based meta-analyses of these studies, the regions correlating with the different formulations of signed RPE have been found to be predominantly subcortical, including the striatum and amygdala, with some cortical regions, such as the ventromedial prefrontal cortex and the cingulate cortex also reported [Bartra et al., 2013; Garrison et al., 2013; Liu et al., 2011]. Additionally, substantial effort has been undertaken to identify how different types of outcomes (primary reward such as food, or secondary reward such as monetary outcomes) can modulate signed RPE in the same regions and the extent to which it can be considered a domain-general, common currency signal [Sescousse et al., 2013].

While using trial-by-trial estimates of signed RPE from reinforcement-learning models has provided an enormously productive framework for understanding learning and decision-making, a growing number of studies have also discussed the complementary role of surprise, namely the unsigned RPE, which can also be estimated at the single-trial level. These include, but are not limited to, the use of trial-by-trial estimates of the modulus of RPE or Bayesian surprise according to Bayesian learning theory [Hayden et al., 2011; Iglesias et al., 2013]. Additionally, human electroencephalography (EEG) studies, attempting to offer a temporal account of the cortical dynamics associated with RPE processing, did not find a systematic monotonic response profile consistent with a single RPE representation but instead offered evidence suggestive of separate representations for valence and surprise at the macroscopic level of responses recorded on the scalp. Specifically, multiple recent EEG studies combining model-based RPE estimates with single-trial analysis of the EEG revealed an early outcome stage reflecting a purely categorical valence signal and a later processing stage reflecting separate representations for valence and surprise [Fouragnan et al., 2015; Fouragnan et al., 2017; Philiastides et al., 2010b]. These later valence and surprise signals appeared in spatially distinct but temporally overlapping EEG signatures.

These findings suggest that, in addition to the fully monotonic firing pattern of midbrain neurons, there exist individual representations for valence and surprise, potentially subserving different functional roles during reward-based learning (e.g. approach-avoidance behavior and the speed of learning via varying degrees of attentional engagement, respectively). Here, we conducted an fMRI meta-analysis to explore the possibility that there exist separate neuronal representations encoding valence and surprise promoting reward learning in humans. We discuss the findings of our work in the context of recent reports from animal neurophysiology and human neuroimaging experiments that provide evidence towards a distributed coding of the different facets of the RPE signal [Brischoux et al., 2009; Fouragnan et al., 2015; Fouragnan et al., 2017; Matsumoto and Hikosaka, 2009].

Materials and Methods

Literature search. We selected fMRI studies using the Pubmed database (http://www.ncbi.nlm.nih.gov/pubmed) with the following search keywords: "(fMRI OR neuroimaging) AND (prediction error OR reward OR surprise)" along with three initial filters preselecting studies in which participants were human adults of over 19 years of age and excluding reviews. This initial selection resulted in 724 candidates for inclusion to which a further twenty papers were added from existing in-house reference libraries. Note that previous meta-analyses used the terms "prediction error" or "reward" but we are the first to include "surprise" in our systematic search for relevant papers [Bartra et al., 2013; Garrison et al., 2013; Sescousse et al., 2013].

Abstracts from the 788 candidate-papers identified were then evaluated for inclusion in the corpus according to the following criteria. We required studies of healthy human adults, reporting changes in BOLD as a function of three different components of RPE: the categorical valence, surprise and signed RPE, including statistical comparisons either in the form of binary contrasts or continuous parametric analyses. Because the main objective of the present meta-analysis is to examine the neural coding of RPE processing at decision outcome, we also imposed the restriction that fMRI analyses were time-locked to the presentation of outcomes (feedback). We used studies involving outcomes consisting of abstract points, monetary payoffs, consumable liquids and arousing pictures but excluded papers in which outcomes consisted of social feedback. We also required that studies used functional brain imaging and did not use pharmacological interventions and ensured that the reported coordinates were either in Montreal Neurological Institute (MNI) or Talairach space. Finally, we excluded papers in which results were derived from region of interest (ROI) since our meta-analytic statistical methods assume that foci are randomly distributed in the whole brain under the null hypothesis. After applying these constraints our meta-analysis

148 comprised 102 publications with a total of 2316 participants, 144 contrasts, and 991
149 activation foci. The number of participants per study ranged from 8 to 66 (median = 24,
150 interquartile range [IQR] = 7).
151
152 ***Study categorization***. The goal of this meta-analysis was to separately categorize studies
153 along the three components of RPE, locked at time of outcome, in order to: 1) identify the
154 extent to which there exist distinct neural representations for valence and surprise and 2)
155 identify whether the neural correlates of the signed RPE simply intersect those of valence
156 and surprise (possibly due to colinearities across these components) or appear as unique
157 clusters of activation reflecting the true combined influence of the two measures.
158
159 To group the relevant papers according to the three main RPE components we used the
160 following definitions: 1) *valence* represents the sign of the RPE and as such it is positive
161 when an outcome is better than expected and negative when worse than expected, 2)
162 *surprise* represents the absolute degree of deviation from expectations and is treated as an
163 unsigned quantity and 3) *signed RPE* simultaneously reflects the influence of both valence
164 and surprise and appears as a fully signed parametric signal. According to these definitions,
165 we identified several fMRI statistical analyses conducted in the original studies that fall under
166 each of the three RPE components (Table 1). The main assumptions of these fMRI
167 analyses, with regard to the BOLD signal as a function of each RPE component, are
168 presented schematically in Figure 1.
169
170 [Figure 1]
171
172 For the valence components, the literature has looked at neural responses which vary
173 categorically along positive-negative axes, as represented in patterns A (i) and (ii) of Figure
174 1. We therefore extracted activations exhibiting a relative BOLD signal increase for negative
175 relative to positive outcomes (NEG > POS: pattern A (i)) and greater BOLD for positive

relative to negative outcomes (POS > NEG: pattern A (ii)), respectively. We considered six types of fMRI statistical comparisons which reported coordinate results from either: (1) a contrast associated with negative > positive outcomes, (2) a contrast associated with negative > no outcomes, (3) a negative correlation with a trial-by-trial regressor modulated by [+1] for positive outcomes and [-1] for negative outcomes, (4) the positive correlation with the regressor described in (3), (5) a contrast associated with positive > negative outcomes and (6) a contrast associated with positive > no outcomes. We grouped results from contrasts 1-3 (i.e. NEG > POS) and contrasts 3-6 (i.e. POS > NEG) to capture regions yielding greater BOLD activity for negative relative to positive outcomes and a greater activity for positive relative to negative outcomes respectively (Table 1).

While the fMRI literature on RPE processing has produced a large amount of theoretical and empirical evidence for the valence and the signed RPE components, comparatively little has been done to directly investigate surprise as a separate component. Fewer studies have used fMRI regressors that were parametrically modulated by trial-to-trial changes in surprise using the unsigned RPE [Fouragnan et al., 2017; Hayden et al., 2011; Iglesias et al., 2013]. These studies used the terms "surprise", "unsigned RPE", or outcome "salience" to refer to the mathematical modulus of RPE from computational learning models. In addition to these papers, our literature search has revealed a number of other measures (see below), which are highly correlated with outcome surprise, as defined by learning theory. We therefore used these measures as proxies of surprise to gain insights into the spatial extent of the relevant neural responses and the degree to which they overlap with those associated with valence.

Specifically, a recent line of research has investigated the neural basis of “Bayesian surprise” or “volatility”, computed as the direct modulus of Bayesian predictive error [Ide et al., 2013; Iglesias et al., 2013; Mathys et al., 2014; O’Reilly et al., 2013] which correspond to the absolute difference between categorical outcomes and the probabilistic expectation of

these outcomes, estimated using Bayesian inference. In the framework of Bayesian learning, the absolute Bayesian RPE plays an important role in learning from rapid changes in behavioral exploration [Courville et al., 2006]. Finally, other studies used the term “associability” which is a parameter in the Pearce-Hall model [Hall and Pearce, 1979; Pearce and Hall, 1980] defined as the degree of divergence between an actual outcome and the original expectation (e.g., the associative strength between a choice and an outcome). We note however, that in the RL framework, associability can also refer to the learning rate. It is clear from these reports that there is a lack of consistent terminology to refer to unsigned RPE, which emphasizes the need for a more unified framework for studying RPE processing.

To test for consistencies in the neuronal responses across these different reports, and provide initial support for a unified representation of surprise, we grouped fMRI analyses which reported outcome-locked activations resulting from: (1) a positive correlation with a trial-by-trial regressor of the modulus (unsigned) RPE resulting from RL models across both positive and negative outcomes ("surprise" or "unsigned RPE"), (2) a positive correlation with a trial-by-trial regressor of the unsigned RPE resulting from Bayesian modelling ("Bayesian Surprise" or "volatility"), (3) a positive correlation with a trial-by-trial regressor of the free parameter of the Pearce-Hall model ("associability" term), (4) a contrast associated with (high positive outcomes and high negative outcomes) > (low positive outcomes and low negative outcomes OR no outcomes, (5) a positive correlation with a parametric regressor of surprising positive RPE alone and (6) a positive correlation with a parametric regressor of surprising negative RPE alone (Table 1). Figure 1 illustrates the hypothesized pattern of BOLD signal predicted by these contrasts (pattern B), exhibiting a V shaped response profile that is maximal for both highly surprising negative and positive RPEs. Despite possible subtle differences in the definition of these measures we expected that only foci consistently correlating with deviations from reward expectations would be revealed in this analysis.

One reason the surprise component has not been looked at closely in isolation is because the literature has focused primarily on signed RPE representations instead. This approach was motivated by neurophysiology experiments showing monotonic responses as a function of both valence and surprise and by a theoretical framework suggesting that learning is driven by a single signed RPE representation. To identify the spatial extent of these representations we also looked at fMRI data reporting positive correlations with signed RPE (negative correlation were discarded). Specifically, we combined four types of fMRI analyses, which estimated trial-by-trial signed RPE from different computational models. We used fMRI reports from (1) model-free and (2) model-based RL methods. Model-free methods include Markov Chain Monte Carlo and temporal difference methods [Samson et al., 2010; Seymour et al., 2007]. Model-based methods include dynamic programming and certainty equivalent methods [Daw et al., 2005; Doya et al., 2002]. More on these algorithms can be found in the review by [Kaelbling et al., 1996]. We also included continuous parametric analyses using trial-by-trial signed RPE from (3) Bayesian RL framework described above [Iglesias et al., 2013; Mathys et al., 2014; den Ouden et al., 2012]. Finally, our analysis for signed RPE also contained one type of parametric analysis that employed fixed RPE values (not estimated from RL models) ranked on a scale such that (4) high positive RPEs > low positive RPEs > low negative RPEs > high negative RPEs (Table 1). Figure 1 illustrates the hypothesized pattern of BOLD signal predicted by these contrasts (pattern C) and it is assumed to increase linearly as a function of signed RPE.

Crucially, we note that an issue requiring closer scrutiny pertains to the difficulty in disambiguating the signed RPE pattern of activity from those associated with valence and surprise. Specifically, pattern C (signed RPE) is generally highly correlated with pattern A (ii), (POS > NEG valence) and in studies in which only positive RPEs are considered, pattern C (signed RPE) and pattern B (surprise) are perfectly correlated. Nonetheless, comparing clusters of activations across the three RPE components could potentially reveal whether or not there exist unique clusters of activations associated with signed RPE.

[Table 1]

2.1. Activation Likelihood Estimation (ALE) analysis

We conducted the meta-analysis using the GingerALE software (version 2.3.6) [Eickhoff et al., 2009] that employs a revised (and rectified [Eickhoff et al., 2017]) version of the activation likelihood estimation (ALE) algorithm [Laird et al., 2005; Turkeltaub et al., 2002], which identifies common areas of activation across studies. This method performs coordinate based meta-analysis which considers each reported foci as a 3D Gaussian probability distribution, centred at the coordinates provided by each study reflecting the spatial uncertainty associated with each reported set of coordinates. Note that each contrast provided to the ALE algorithm is treated as a separate experiment. The probabilities distributions are then combined to create a modelled activation map, namely an ALE map for that contrast. Studies are weighted according to the number of subjects they contain by adjusting the full width at half maximum of the Gaussian distributions. The convergence of results across the whole brain is obtained by computing the union of all resulting voxel-wise ALE scores. To distinguish meaningful convergence from random noise, statistics are computed by comparing ALE scores with an empirical null-distribution representing a random spatial association between studies. To infer true convergence, a random-effect inference is applied to capitalize on the differences between studies rather than between foci within a particular study. The null-hypothesis is modelled by randomly sampling voxels from each of the ALE maps from which the union is obtained. The ALE maps are assessed against the null distribution using a cluster level threshold of specific p-values. Contrast analyses between categories of the entire dataset are determined by ALE subtraction method, including a correction for differences in sample size between the categories.

Here, we manually extracted all coordinates from the studies shown in Table 1 and entered them into separate files for each of the three RPE components in preparation for the ALE analyses. Any studies that provided coordinates in Talairach space were converted into MNI space by the Matlab (MathWorks, Natick, Massachusetts) function *tal2mni* in the fieldtrip toolbox [Oostenveld et al., 2011]. We conducted ALE analyses for each of the three components of RPE individually. Along the valence component, we looked at both patterns A (i) and A (ii) in Figure 1 (i.e. to identify activations for negative > positive RPE and vice versa, respectively). Accordingly, we ran separate ALE analyses for each of the two patterns. In addition, we performed two conjunction analyses – one between the valence and surprise components to investigate our hypothesis of largely separate neural representations and another between all three RPE components to identify regions that simultaneously encode these representations. Subsequently, we also performed all possible pairwise contrast analyses between the three patterns (A, B and C), using the individual maps associated with each pattern.

A total of 402 foci from 66 contrasts were used with 262 foci from 31 contrasts for Pattern A (i) revealing BOLD patterns greater for negative than positive outcomes and 205 from 35 contrasts for Pattern A (ii) (e.g. the opposite contrast). For the surprise (Pattern B) and signed RPE (Pattern C) analyses, we applied individual ALE analyses, with 284 foci from 40 contrasts for surprise and 240 foci from 38 contrasts for signed RPE. Overall, the number of contrasts used for each separate outcome component was large enough (> 30) to allow sufficient power for the required statistical tests [Eickhoff and Etkin, 2016]. Finally, we transformed the resulting ALE maps from the Colins MNI individual brain space (Colin27_T1_seg_MNI) to the MNI normalized brain space (MNI ICBM152 template) by applying an affine transformation using the FSL *flirt* program [Jenkinson et al., 2002], prior to overlaying onto the canonical MNI template for visualization.

3. Results

All coordinates used for the following ALE analyses were collated from fMRI studies in which the components of RPE have been regressed onto BOLD activity time-locked to outcome presentation. We report ALE maps with clusters surviving the False Discovery Rate (FDR) yielding two p-value thresholds. The most conservative FDR correction yields a p-value with no assumptions about how the data is correlated (FRN), and the least conservative FDR correction assumes independence or positive dependence (FID) with $p < 0.05$ and a minimum volume clustering value of 50 mm^3. Note that, using a cluster-level family-wise error (FWE) correction implemented with a cluster-extent threshold of $p < 0.05$ and a cluster-forming threshold of $p < 0.001$ revealed virtually identical results (compared with FRN) [Eickhoff et al., 2017] as per previous reports [R Garrison et al., 2017]. For all tables presenting ALE cluster results, the size of each cluster is provided in mm^3 along with the associated MNI coordinates and maximum ALE score. The ALE score indicates the relative effect size for each peak voxel within each ALE analysis.

3.1. Outcome Valence

The first two ALE analyses were conducted to identify regions in which BOLD signals correlate with outcome valence. Specifically, we looked at activations that yielded greater BOLD for negative relative to positive outcomes (NEG > POS; pattern A (i) in Figure 1) and greater BOLD for negative relative to positive outcomes (POS > NEG; pattern A (ii) in Figure 1), respectively. Accordingly, we considered all fMRI studies, which assumed BOLD responses varying categorically along a positive-negative axis for outcome valence.

The findings of the two valence ALE analyses are shown in Figure 2. The resulting maps revealed a highly distributed network of brain activations encompassing several cortical regions and sub-cortical structures. More precisely, NEG > POS valence clusters were found

in a network encompassing the anterior and dorsal part of the mid-cingulate cortex (aMCC and dMCC) including the pre supplementary motor area (pre-SMA), the bilateral anterior and middle insular cortex (aINS, mINS), the bilateral dorsolateral prefrontal cortex (dlPFC), the bilateral thalamus, right amygdala, left inferior parietal lobule (IPL) and the habenula.

POS > NEG valence clusters were found in the bilateral ventral striatum (vSTR), the ventromedial prefrontal cortex (vmPFC), the posterior part of the cingulate cortex (PCC), as well as the ventrolateral orbitofrontal cortex (vlOFC). At a lower threshold (uncorrected p-value of 0.001), we also found the midbrain as part of this network, encompassing the VTA, which is commonly associated with the delivery of reward [D'Ardenne et al., 2008]. Table 2 contains the complete list of regions, coordinates, and statistics of these two ALE analyses.

[Figure 2], [Table 2]

3.2. Surprise

FMRI investigations of RPE have focused primarily on the valence components while neglecting potential *c*ontributions from possible separate representations along the surprise component, defined as the degree by which outcomes deviate from expectations and mathematically expressed as the modulus of RPE. A major goal of this work was to explore the possibility that there exist largely separate neuronal representations encoding surprise. To this end, we conducted a new ALE analysis in which the few empirical fMRI studies making use of the surprise from RL models were combined with other fMRI measures correlated with the surprise as defined by RL models (Table 1).

Figure 3 shows the areas in which BOLD signal correlated with surprise. We found evidence for activations in a distributed network encompassing the aMCC, dMCC, the pre-SMA the bilateral dorsal striatum (dSTR), the bilateral aINS, the MTG and the midbrain. Crucially, this

activation map shows that the neural network associated with surprise is largely distinct from that of valence. This finding provides initial support for the notion that these two RPE components are encoded in separate brain areas and, as such, they might be contributing individually to promote learning. The full results of the surprise ALE analysis are also summarized in Table 3.

[Figure 3], [Table 3]

3.3. Valence and surprise conjunction and contrast analyses

The activation maps for valence (NEG > POS and POS > NEG) and surprise ALE analyses conducted above revealed little overlap between the spatial representations of these two RPE components. To formally quantify the degree of overlap between the valence and surprise networks, we next ran a conjunction analysis between the two components. The statistical map resulting from this conjunction analysis and the two separate statistical maps of valence and surprise (as already reported in Figures 2 and 3) are overlaid in Figure 4.

[Figure 4], [Table 4]

Contrast analyses were conducted for each possible pairing between any dimensions of valence (POS > NEG [positive]; NEG > POS [negative] and POS + NEG [all valence]) and surprise. These analyses allowed us to identify the areas that were unique and specific to each individual outcome and RPE-related component. The positive valence (pattern A (ii)) minus surprise (pattern B) contrast revealed two main clusters in the vSTR and vmPFC whereas the reverse contrast revealed a network of clusters including preSMA, aINS, and MTG. Contrasting negative valence (pattern A (i)) and surprise also exposed separate networks of areas for each subtraction. Specifically, this contrast revealed a network encompassing the thalamus, the habenula, the right mINS and the dMCC, whereas the

reverse contrast showed clusters in the dorsal portion of the STR and the dlPFC. The statistical maps resulting from these contrast analyses are presented in Figure 5.

[Figure 5], [Table 5]

3.4. Signed RPE

A major goal of this work was to investigate the spatial profile of the signed RPE component and to scrutinise more closely the extent to which it overlaps with the separate representations identified for valence (NEG > POS and POS > NEG) and surprise. The fMRI-RPE literature has focused on this component largely due to neurophysiological evidence suggesting that RPE-like learning is driven by a single, theoretically unified representation of both POS > NEG valence and surprise (Table 1).

Results from this ALE analysis revealed very few unique activations for signed RPE compared to valence and surprise. Instead, brain areas identified in this analysis overlapped mostly with areas appearing in the POS > NEG valence component and, to a lesser extent, surprise (Figure 6). Specifically, a large overlap between signed RPE and the POS > NEG valence component was found in the STR and a smaller one in the vmPFC. Similarly, areas appearing in the singed RPE analysis that overlapped with the surprise component were also found, albeit only in small clusters comprising the aMCC and dorsal STR. Taken together, these findings emphasize the potential collinearities between the BOLD predictors used to identify neural representations associated with the three RPE components and highlight the need for developing a methodology for properly disentangling their individual contributions.

[Figure 6], [Table 6]

3.5. Putting it all together

Subsequently, to formally test for the overlap between all three RPE components and identify potential regions integrating valence and surprise either into a signed RPE representation or a linear superposition of the two signals [Fouragnan et al., 2017], we performed a conjunction analysis between the valence (pattern A), the surprise (pattern B) and signed RPE (pattern C) signals. We summarize our conjunction results in Figure 7, which revealed a major overlap between all activations associated with signed RPE and each of the other two RPE representations in the central part of the STR. Thus, one possibility is that the STR meets the requirement that a full monotonic representation of the error signal also simultaneously encodes valence and surprise, as per our last ALE analysis.

[Figure 7]

Another possibility is that the overlap between all components of outcomes in the STR is arising, at least in part, due to collinearities across the different outcome representations, particularly between the positive categorical nature of outcome valence (pattern A (ii)) and the signed RPE. To formally test this hypothesis, we performed a new series of contrast analyses between signed RPE and all dimensions of categorical valence and surprise. Particularly, we performed contrast analyses between patterns C-A(i), C-A(ii), C-A and C-B (and vice versa). The results are summarized in Figure 8. Particularly, we did not find any area unique to signed RPE when looking at each of the individual comparisons of signed RPE with the other three patterns. In fact, when comparing signed RPE to positive valence (pattern A (ii)), no clusters were found to be significantly different than those found with the categorical outcome valence (POS > NEG). Conversely, the STR was found for all the other signed RPE comparisons (signed RPE > negative; signed RPE > surprise). Finally, the unique network related to negative valence (pattern A (i)) was found in the dMCC, thalamus

and mINS, the unique cluster related to positive valence was found in the vmPFC and the unique network related to surprise was found in the aMCC, preSMA and the aINS.

[Figure 8], [table 7]

Discussion

In this fMRI meta-analysis work, we demonstrated that reward learning in humans involves separate neuronal signatures of RPE, comprising distinct representations for valence and surprise. Together with recent neurophysiological and EEG evidence (including studies using simultaneous EEG and fMRI), these findings point to a potentially sequential and distributed encoding of different RPE components with potentially functionally distinct roles.

Valence networks

The ALE analyses related to valence revealed two distributed set of activations correlating with both pattern A (i) and (ii) in Figure 1. Foci for which the BOLD signal was greater for negative than positive outcomes showed significant clustering in a large network of areas including the thalamus, the aMCC and dMCC, the aINS, mINS and the dlPFC. Conversely, foci for which the BOLD signal was greater for positive than negative outcomes showed significant clusters in a separate network including vmPFC, vSTR, PCC, and vlOFC. These findings clearly suggest the presence of multiple systems responding to the categorical nature of valence which supports the notion that separate valuation systems shape learning in the human brain [Fiorillo, 2013; Fouragnan et al., 2013], although their functional role remain debated. More specifically, the debate focuses on the number and exact nature of the neural systems assigning value to decision outcomes and driving behaviors that are evolutionarily appropriate in response to changes in the environment.

A first theory describes two distinct valence systems invoking two orthogonal axes of decision-making: alertness (involving the implementation of action) and learning (including the updates of value expectations for future avoidance and approach behaviors). In this framework, the first system is thought to monitor on-going activity and interrupt it when needed to trigger switching behaviors (e.g. following negative RPEs). In contrast, the second system uses both negative and positive RPE values for decreasing or increasing internal value representations associated with decisions to ultimately drive avoidance and approach learning, respectively [Boureau and Dayan, 2011; Cools et al., 2011; Elliot, 2006; Fiorillo, 2013; Fouragnan et al., 2015; Gray and McNaughton, 2003; Guitart-Masip et al., 2012].

A second (not mutually exclusive) proposition supports the idea that there are at least two separate systems responsible for aversive and appetitive reinforcements such that punishments and rewards are encoded separately (i.e. a punishment space and a reward space [Morrens, 2014]). This proposition was developed on the basis of neurophysiological evidence showing that different types of neurons exhibit differential activity in response to punishing vs. non-punishing outcomes and rewarding vs. non-rewarding outcomes, respectively [Fiorillo et al., 2003; Fiorillo, 2013; Schultz et al., 1992; Schultz, 1998]. In this second theory, the punishment space is responsible for avoidance behaviors as well as avoidance learning and the reward space is responsible for approach behaviors and approach learning.

It is noteworthy that our meta-analysis on itself cannot directly distinguish between the two theories because the results do not reveal whether the relevant activations respond exclusively to either positive or negative outcomes or are modulated by both outcomes in opposite directions. This distinction is critical because the former response profile would suggest the presence of separate approach and avoidance systems that might not necessarily be linked to the learning processes as such, while the latter might point to both up- and down-regulation of activity consistent with learning and updating of reward

expectations. Nonetheless, the meta-analysis results suggest that two main networks process valence. The network encompassing aINS, aMCC, thalamus and dlPFC could regulate on-going activity and alertness or could represent the punishment space in accordance to the first and the second theories respectively. Conversely, the network of regions encompassing the vmPFC, vSTR, PCC and vlOFC could represent the learning system depicted in the first theory or could represent the reward space depicted in the second theory. Further research is required to tease apart the roles of these systems, especially by investigating their precise response profiles in the appetitive (where rewarding and non-rewarding outcomes are manipulated) and in a true aversive (where punishing and non-punishing outcomes are manipulated) domains, respectively.

Surprise network

Emerging evidence indicates that the brain encodes the unsigned RPE signal (surprise), which alerts the organism of relative deviations from expectations, regardless of the outcome value. However, to date, only few papers have modelled surprise as such to search for independent neural representations, with the exception of recent neurophysiological developments [Brischoux et al., 2009; Matsumoto and Hikosaka, 2009], recent EEG work [Philiastides et al., 2010b; Yeung and Sanfey, 2004] and an increasing number of fMRI studies [Fouragnan et al., 2017; Gläscher et al., 2010; Li and Daw, 2011; Metereau and Dreher, 2013]. Nevertheless, other fMRI studies used variables highly correlated with surprise that can be employed as proxies [Behrens et al., 2007; Iglesias et al., 2013; Nassar et al., 2012; den Ouden et al., 2012; Yu and Dayan, 2005]. These studies share the assumption that the corresponding BOLD response profile is maximal for high positive and high negative RPE and minimal for no RPE, resembling a V-shape, as illustrated with Pattern B in Figure 1. By combining these fMRI results into a single ALE-analysis, we expose for the first time the network associated with surprise while stressing the need for a common lexicon for this learning component to guide subsequent research in the field.

The surprise ALE-analysis revealed a large network including cortical and sub-cortical areas such as aMCC, bilateral aINS, dSTR and midbrain, that differed majoritarily from those of valence processing although small overlaps were found between the two components at the junction of ventral and dorsal STR, in left aINS and aMCC. Importantly, the role of surprise is still a subject of debate. Some studies propose that this network encodes the saliency of an outcome or how much a stimulus stands out from others [Litt et al., 2011; Zink et al., 2004]. As such, the surprise system could be considered as a key attentional mechanism that enables an organism to focus its limited perceptual and cognitive resources on the most pertinent subset of the available sensory data, similarly to the attentional mechanism used to guide decisions in the case of salient stimuli [Kahnt and Tobler, 2013]. Consistent with a role in attention regulation, representations of such signal have been found in lower-level visual areas [Serences, 2008], lateral intraparietal cortex [Huettel et al., 2006; Kahnt and Tobler, 2013] and areas involved in visual and motor preparation such as the supplementary motor area [Wunderlich et al., 2009] or the supplementary eye field [Middlebrooks and Sommer, 2012; So and Stuphorn, 2012].

In contrast, it has also been suggested that a surprise system can independently monitor unexpected information and act as a learning signal that allows better predictions of upcoming events, and help plan appropriate behavioral adjustments [Dayan and Balleine, 2002; Fouragnan et al., 2017; Kolling et al., 2012; Wittmann et al., 2016]. In particular, some studies suggest that the aINS receives information related to surprise and direct modulation from the dSTR providing crucial information for behavioral adjustment [Menon and Levitin, 2005]. Along these lines, the surprise signal also captures the essence of a learning signal that the brain needs to compute to maintain a homeostatic state [Friston et al., 2006; Friston, 2009]. Practically, this means that the brain elaborates internal predictions about sensory input and updates them according to surprise, a process that can be formulated as generalized Bayesian filtering or predictive coding in the brain. Finally, still in the framework

564 of learning, some authors argue that surprise can also be considered as a signal predicting
565 the level of risk associated with a future decision outcome, and thus reflect a risk RPE
566 [Fiorillo et al., 2003; Preuschoff et al., 2008; Rudorf et al., 2012].
567
568 **Neuromodulatory pathways encoding multicomponent RPE signals**
569
570 Supporting the idea of separate neural systems for valence and surprise, recent
571 electrophysiological work has revealed both signals existing in neighbouring groups of
572 neurons. The first study of this kind observed the response of dopaminergic neurons in
573 ventral and dorsal areas of the SNc and reported two categories of dopamine neurons
574 [Matsumoto and Hikosaka, 2009]. Some dopamine neurons increase their phasic firing
575 activity in response to valence while others responded only to the changes in unsigned RPE,
576 regardless of the valence component. The latter population of neurons was located more
577 dorsolaterally in the SNc, whilst the neurons encoding valence were located more
578 ventromedially, including the VTA. Interestingly, the dorsolateral SNc projects mainly to the
579 dorsal STR, whereas the ventral SNc and VTA project to the ventral STR, which matches
580 the results of our last conjunction analysis (Figure 7). We found that the only region that
581 encodes the full monotonic representation of the RPE as well as the separate valence and
582 surprise components of RPE seems to be the central part of the STR as shown in Figure 7.
583 This result aligns with the assumption that this region receives direct projections from the
584 midbrain dopaminergic neurons encoding a fully monotonic signed RPE signal [Schultz et
585 al., 1997]. Additionally, the meta-analysis also revealed that both the valence (POS > NEG)
586 and surprise networks include activity in the midbrain, confirming this hypothesis.
587
588 It is important to note that identifying neural activity associated with valence and surprise
589 signals is challenging because in many experimental paradigms both components are highly
590 correlated. For example, when positive RPE are manipulated in isolation, valence (POS >
591 NEG) strongly correlates with surprise. Additionally, whether positive or negative, an

592 unexpected outcome attracts more attention, leads to higher levels of emotional arousal and
593 involves higher levels of motor preparation compared to no RPE [Matsumoto and Hikosaka,
594 2009; Maunsell, 2004; Roesch and Olson, 2004]. Consequently, to disentangle these
595 signals, one needs to design tasks in which the level of valence and surprise can
596 independently be controlled and decoupled [Kahnt, 2017; Kahnt and Tobler, 2013] or
597 capitalize on the variability of physiologically-derived responses (i.e. endogenous variability)
598 associated with valence and surprise [Fouragnan et al., 2015; Fouragnan et al., 2017;
599 Pisauro et al., 2017].
600
601 It is important to note that since the problem of collinearity and functional specificity of some
602 brain regions is already present in single studies, it will inevitably be carried over to studies
603 performing conjunction meta-analyses. Virtually every experimental design engages a large
604 number of cognitive operations and, thereby, activates functional neural networks that may
605 be irrelevant to a particular regressor (psychological construct) of interest. For example in
606 our study, regions related to outcome value and surprise might share variance with outcome
607 confidence [Gherman and Philiastides, 2015; Gherman and Philiastides, 2017; Lebreton et
608 al., 2015; Philiastides et al., 2014]. Despite this general limitation and the difficulty of
609 interpreting conjunction results, aggregating results across a large number of experiments
610 allows one to expose convergence of findings across studies and increasing the
611 generalizability of the conclusions. In particular, this meta-analysis, capitalizing on both
612 individual maps of activations as well as contrasts between different outcome components,
613 points to a distributed encoding of valence and surprise, with potentially distinct functional
614 roles.
615
616 **Temporally specific components of RPE processing**
617
618 The presence of separate RPE-related neural systems raises the question of how these
619 systems unfold in time. Capitalizing on the high temporal resolution of EEG, three recent

studies using simultaneous EEG-fMRI have started to shed light on the spatiotemporal characterisation of the RPE components. First, these studies have revealed two temporally specific EEG components discriminating between positive and negative RPEs peaking around 220ms and 300ms respectively, largely consistent with the timing of the feedback-related negativity and feedback-related positivity ERP components [Cohen et al., 2007; Hajcak et al., 2006; Yeung and Sanfey, 2004]. Additionally, the studies also revealed a late unsigned RPE component which overlaps temporally with the late valence signal [Philiastides et al., 2010b] but appears in a largely separate and distributed neural network [Fouragnan et al., 2017].

Based on these previous studies and the current meta-analysis, we propose that the early and late EEG valence components might reflect the separate contributions of the two networks of areas found for the ALE-valence analyses. This proposal assumes that an early network processes mainly negative RPEs in order to initiate a fast alertness response in the presence of negative outcomes. Conversely, a later network – associated with the brain's reward circuitry – is modulated by both positive and negative RPEs, consistent with a role in approach/avoidance learning and value updating [Philiastides et al., 2010a]. We also propose that the surprise network unfolds near simultaneously with the late valence component and thus influences learning through largely distinct spatial representations of the two outcomes signals, which happen to form a composite signal in overlapping areas [Fouragnan et al., 2017].

Full representation of a monotonic signed RPE signal

To examine the spatial profile of a true monotonic signed RPE representation in the human brain, we pooled results from fMRI studies, which hypothesized that RPE-like learning is driven by a simultaneous representation of both categorical valence and surprise. These

fMRI studies are based on the influential assumption that BOLD signal increases monotonically as a function of signed RPE, as illustrated in pattern C (Fig. 1), equivalent to the teaching signal that is predicted in the Rescorla–Wagner model of RL [Rescorla and Wagner, 1972]. Additionally, we combined the valence and surprise networks and subsequently compared it with the signed RPE to test the requirement that the signed RPE simultaneous encodes both components. This conjunction analysis revealed that the only brain region that seems to encode a true monotonic signal is the STR in the basal ganglia, which could explain why such a signal is not tractable with EEG recordings as highlighted earlier. This result confirms the long standing view that the BOLD activity in STR mirrors the dopaminergic signalling of the mesolimbic neurons [Delgado et al., 2000; Haber et al., 1995; O'Doherty et al., 2004; Pagnoni et al., 2002] that fully encode the RL prediction error signal of the Rescorla-Wagner rule [Ikemoto, 2007; Schultz et al., 1992].

Nonetheless, the ALE contrast analyses between valence (the positive correlation with pattern A (ii)) and signed RPE revealed no significant activation, whereas the reverse contrast revealed a denser cluster of activity in vmPFC for valence than signed RPE. Given the evidence presented above that the signed RPE may only be encoded in the STR, we suggest that this result may arise due to collinearities between valence and signed RPE or surprise and signed RPE. More precisely, a parametric predictor for signed RPE would be positively correlated with the contrast positive > negative outcomes whereas the signed RPE and surprise would be perfectly correlated in the positive (appetitive) domain.

Conclusion

In conclusion, the current meta-analysis points to a framework whereby heterogeneous signals are involved in RPE processing. The proposal of a temporally distinct and spatially distributed representation of valence and surprise is open to debate and many questions remain about how these signals interact and how they correspond to the computations made

675 in the brain. For example, it is currently unclear whether valence and surprise encoding
676 occur before the computation of the signed RPE, or whether these three computations are
677 performed in parallel. Nevertheless the taxonomy proposed is conceptually useful because it
678 breaks down the learning and valuation processes into testable components and organizes
679 the RPE literature in terms of the computations that are potentially involved. It will require
680 additional experiments to validate the current proposal and to better understand the
681 complexity of RPE processing.
682

683 **References**

684 Abler B, Walter H, Erk S, Kammerer H, Spitzer M (2006): Prediction error as a linear function
685 of reward probability is coded in human nucleus accumbens. NeuroImage 31:790–
686 795.
687 Allen M, Fardo F, Dietz MJ, Hillebrandt H, Friston KJ, Rees G, Roepstorff A (2016): Anterior
688 insula coordinates hierarchical processing of tactile mismatch responses.
689 NeuroImage 127:34–43.
690 Amado C, Hermann P, Kovács P, Grotheer M, Vidnyánszky Z, Kovács G (2016): The
691 contribution of surprise to the prediction based modulation of fMRI responses.
692 Neuropsychologia 84:105–112.
693 Amiez C, Sallet J, Procyk E, Petrides M (2012): Modulation of feedback related activity in the
694 rostral anterior cingulate cortex during trial and error exploration. NeuroImage
695 63:1078–1090.
696 Aron AR, Shohamy D, Clark J, Myers C, Gluck MA, Poldrack RA (2004): Human Midbrain
697 Sensitivity to Cognitive Feedback and Uncertainty During Classification Learning. J
698 Neurophysiol 92:1144–1152.
699 Bartra O, McGuire JT, Kable JW (2013): The valuation system: a coordinate-based meta-
700 analysis of BOLD fMRI experiments examining neural correlates of subjective value.
701 NeuroImage 76:412–427.
702 Behrens TEJ, Woolrich MW, Walton ME, Rushworth MFS (2007): Learning the value of
703 information in an uncertain world. Nat Neurosci 10:1214–1221.
704 Bickel WK, Pitcock JA, Yi R, Angtuaco EJC (2009): Congruence of BOLD Response across
705 Intertemporal Choice Conditions: Fictive and Real Money Gains and Losses. J
706 Neurosci 29:8839–8846.
707 Boll S, Gamer M, Gluth S, Finsterbusch J, Büchel C (2013): Separate amygdala subregions
708 signal surprise and predictiveness during associative fear learning in humans. Eur J
709 Neurosci 37:758–767.
710 van den Bos W, Cohen MX, Kahnt T, Crone EA (2012): Striatum-medial prefrontal cortex
711 connectivity predicts developmental changes in reinforcement learning. Cereb
712 Cortex N Y N 1991 22:1247–1255.
713 Boureau Y-L, Dayan P (2011): Opponency Revisited: Competition and Cooperation Between
714 Dopamine and Serotonin. Neuropsychopharmacology 36:74–97.
715 Brischoux F, Chakraborty S, Brierley DI, Ungless MA (2009): Phasic excitation of dopamine
716 neurons in ventral VTA by noxious stimuli. Proc Natl Acad Sci U S A 106:4894–4899.
717 Browning M, Holmes EA, Murphy SE, Goodwin GM, Harmer CJ (2010): Lateral Prefrontal
718 Cortex Mediates the Cognitive Modification of Attentional Bias. Biol Psychiatry
719 67:919–925.
720 de Bruijn E, de Lange F, Cramon D, Ullsperger M (2009): When Errors Are Rewarding. J
721 Neurosci Off J Soc Neurosci 29:12183–6.
722 Canessa N, Crespi C, Motterlini M, Baud-Bovy G, Chierchia G, Pantaleo G, Tettamanti M,
723 Cappa SF (2013): The Functional and Structural Neural Basis of Individual Differences
724 in Loss Aversion. J Neurosci 33:14307–14317.
725 Chumbley JR, Burke CJ, Stephan KE, Friston KJ, Tobler PN, Fehr E (2014): Surprise beyond
726 prediction error. Hum Brain Mapp 35:4805–4814.

727 Cohen MX, Elger CE, Ranganath C (2007): Reward Expectation Modulates Feedback-Related
728 Negativity and EEG Spectra. NeuroImage 35:968–978.
729 Cohen MX, Ranganath C (2007): Reinforcement Learning Signals Predict Future Decisions. J
730 Neurosci 27:371–378.
731 Collins AGE, Frank MJ (2016): Surprise! Dopamine signals mix action, value and error. Nat
732 Neurosci 19:3–5.
733 Cools R, Nakamura K, Daw ND (2011): Serotonin and Dopamine: Unifying Affective,
734 Activational, and Decision Functions. Neuropsychopharmacology 36:98–113.
735 Courville AC, Daw ND, Touretzky DS (2006): Bayesian theories of conditioning in a changing
736 world. Trends Cogn Sci 10:294–300.
737 Daniel R, Wagner G, Koch K, Reichenbach JR, Sauer H, Schlösser RGM (2011): Assessing the
738 neural basis of uncertainty in perceptual category learning through varying levels of
739 distortion. J Cogn Neurosci 23:1781–1793.
740 D'Ardenne K, McClure SM, Nystrom LE, Cohen JD (2008): BOLD responses reflecting
741 dopaminergic signals in the human ventral tegmental area. Science 319:1264–1267.
742 Daw ND, Niv Y, Dayan P (2005): Uncertainty-based competition between prefrontal and
743 dorsolateral striatal systems for behavioral control. Nat Neurosci 8:1704–1711.
744 Daw ND, Gershman SJ, Seymour B, Dayan P, Dolan RJ (2011): Model-Based Influences on
745 Humans' Choices and Striatal Prediction Errors. Neuron 69:1204–1215.
746 Dayan P, Balleine BW (2002): Reward, motivation, and reinforcement learning. Neuron
747 36:285–298.
748 Delgado MR, Nystrom LE, Fissell C, Noll DC, Fiez JA (2000): Tracking the Hemodynamic
749 Responses to Reward and Punishment in the Striatum. J Neurophysiol 84:3072–
750 3077.
751 Delgado MR (2007): Reward-Related Responses in the Human Striatum. Ann N Y Acad Sci
752 1104:70–88.
753 Demos KE, Heatherton TF, Kelley WM (2012): Individual Differences in Nucleus Accumbens
754 Activity to Food and Sexual Images Predict Weight Gain and Sexual Behavior. J
755 Neurosci 32:5549–5552.
756 Diederen KMJ, Ziauddeen H, Vestergaard MD, Spencer T, Schultz W, Fletcher PC (2017):
757 Dopamine Modulates Adaptive Prediction Error Coding in the Human Midbrain and
758 Striatum. J Neurosci Off J Soc Neurosci 37:1708–1720.
759 Diuk C, Tsai K, Wallis J, Botvinick M, Niv Y (2013): Hierarchical Learning Induces Two
760 Simultaneous, But Separable, Prediction Errors in Human Basal Ganglia. J Neurosci
761 33:5797–5805.
762 Doya K, Samejima K, Katagiri K, Kawato M (2002): Multiple model-based reinforcement
763 learning. Neural Comput 14:1347–1369.
764 Dreher J-C (2013): Neural coding of computational factors affecting decision making. Prog
765 Brain Res 202:289–320.
766 van Duijvenvoorde ACK, Op de Macks ZA, Overgaauw S, Gunther Moor B, Dahl RE, Crone EA
767 (2014): A cross-sectional and longitudinal analysis of reward-related brain activation:
768 Effects of age, pubertal stage, and reward sensitivity. Brain Cogn 89:3–14.
769 Dunne S, D'Souza A, O'Doherty JP (2016): The involvement of model-based but not model-
770 free learning signals during observational reward learning in the absence of choice. J
771 Neurophysiol 115:3195–3203.
772 Eickhoff SB, Etkin A (2016): Going Beyond Finding the "Lesion": A Path for Maturation of
773 Neuroimaging. Am J Psychiatry 173:302–303.

Eickhoff SB, Laird AR, Fox PM, Lancaster JL, Fox PT (2017): Implementation errors in the GingerALE Software: Description and recommendations. Hum Brain Mapp 38:7–11.
Eickhoff SB, Laird AR, Grefkes C, Wang LE, Zilles K, Fox PT (2009): Coordinate-based activation likelihood estimation meta-analysis of neuroimaging data: a random-effects approach based on empirical estimates of spatial uncertainty. Hum Brain Mapp 30:2907–2926.
Elliot AJ (2006): The Hierarchical Model of Approach-Avoidance Motivation. Motiv Emot 30:111–116.
Elliott R, Friston KJ, Dolan RJ (2000): Dissociable neural responses in human reward systems. J Neurosci Off J Soc Neurosci 20:6159–6165.
Elward RL, Vilberg KL, Rugg MD (2015): Motivated Memories: Effects of Reward and Recollection in the Core Recollection Network and Beyond. Cereb Cortex 25:3159–3166.
Ernst M, Nelson EE, McClure EB, Monk CS, Munson S, Eshel N, Zarahn E, Leibenluft E, Zametkin A, Towbin K, Blair J, Charney D, Pine DS (2004): Choice selection and reward anticipation: an fMRI study. Neuropsychologia 42:1585–1597.
Ferdinand NK, Opitz B (2014): Different aspects of performance feedback engage different brain areas: Disentangling valence and expectancy in feedback processing. Sci Rep 4:srep05986.
Fiorillo CD (2013): Two Dimensions of Value: Dopamine Neurons Represent Reward But Not Aversiveness. Science 341:546–549.
Fiorillo CD, Tobler PN, Schultz W (2003): Discrete Coding of Reward Probability and Uncertainty by Dopamine Neurons. Science 299:1898–1902.
Forster SE, Brown JW (2011): Medial prefrontal cortex predicts and evaluates the timing of action outcomes. NeuroImage 55:253–265.
Fouragnan E, Chierchia G, Greiner S, Neveu R, Avesani P, Coricelli G (2013): Reputational Priors Magnify Striatal Responses to Violations of Trust. J Neurosci 33:3602–3611.
Fouragnan E, Queirazza F, Retzler C, Mullinger K, Philiastides M (2017): Spatiotemporal neural characterization of prediction error valence and surprise during reward learning in humans. Sci Rep. https://www.nature.com/srep/.
Fouragnan E, Retzler C, Mullinger K, Philiastides MG (2015): Two spatiotemporally distinct value systems shape reward-based learning in the human brain. Nat Commun 6:8107.
Frank MJ, Seeberger LC, O'reilly RC (2004): By carrot or by stick: cognitive reinforcement learning in parkinsonism. Science 306:1940–1943.
Friston K (2009): The free-energy principle: a rough guide to the brain? Trends Cogn Sci 13:293–301.
Friston K, Kilner J, Harrison L (2006): A free energy principle for the brain. J Physiol Paris 100:70–87.
Fujiwara J, Tobler PN, Taira M, Iijima T, Tsutsui K-I (2009): Segregated and integrated coding of reward and punishment in the cingulate cortex. J Neurophysiol 101:3284–3293.
Garrison J, Erdeniz B, Done J (2013): Prediction error in reinforcement learning: A meta-analysis of neuroimaging studies. Neurosci Biobehav Rev 37:1297–1310.
Gherman S, Philiastides MG (2015): Neural representations of confidence emerge from the process of decision formation during perceptual choices. NeuroImage 106:134–143.
Gherman S, Philiastides MG (2017): Human VMPFC encodes early signatures of confidence in perceptual decisions. bioRxiv:224337.

821 Gläscher J, Daw N, Dayan P, O'Doherty JP (2010): States versus rewards: dissociable neural
822 prediction error signals underlying model-based and model-free reinforcement
823 learning. Neuron 66:585–595.
824 Gläscher J, Hampton AN, O'Doherty JP (2009): Determining a Role for Ventromedial
825 Prefrontal Cortex in Encoding Action-Based Value Signals During Reward-Related
826 Decision Making. Cereb Cortex 19:483–495.
827 Gray JA, McNaughton N (2003): The Neuropsychology of Anxiety: An Enquiry Into the
828 Function of the Septo-hippocampal System. Oxford University Press.
829 Guitart-Masip M, Huys QJM, Fuentemilla L, Dayan P, Duzel E, Dolan RJ (2012): Go and no-go
830 learning in reward and punishment: interactions between affect and effect.
831 NeuroImage 62:154–166.
832 Guo R, Böhmer W, Hebart M, Chien S, Sommer T, Obermayer K, Gläscher J (2016):
833 Interaction of Instrumental and Goal-Directed Learning Modulates Prediction Error
834 Representations in the Ventral Striatum. J Neurosci 36:12650–12660.
835 Haber SN, Kunishio K, Mizobuchi M, Lynd-Balta E (1995): The orbital and medial prefrontal
836 circuit through the primate basal ganglia. J Neurosci Off J Soc Neurosci 15:4851–
837 4867.
838 Hajcak G, Moser JS, Holroyd CB, Simons RF (2006): The feedback-related negativity reflects
839 the binary evaluation of good versus bad outcomes. Biol Psychol 71:148–154.
840 Hall G, Pearce JM (1979): Latent inhibition of a CS during CS-US pairings. J Exp Psychol Anim
841 Behav Process 5:31–42.
842 Hare TA, O'Doherty J, Camerer CF, Schultz W, Rangel A (2008): Dissociating the Role of the
843 Orbitofrontal Cortex and the Striatum in the Computation of Goal Values and
844 Prediction Errors. J Neurosci 28:5623–5630.
845 Haruno M, Kuroda T, Doya K, Toyama K, Kimura M, Samejima K, Imamizu H, Kawato M
846 (2004): A neural correlate of reward-based behavioral learning in caudate nucleus: a
847 functional magnetic resonance imaging study of a stochastic decision task. J Neurosci
848 Off J Soc Neurosci 24:1660–1665.
849 Häusler AN, Oroz Artigas S, Trautner P, Weber B (2016): Gain- and Loss-Related Brain
850 Activation Are Associated with Information Search Differences in Risky Gambles: An
851 fMRI and Eye-Tracking Study. eNeuro 3.
852 https://www.ncbi.nlm.nih.gov/pmc/articles/PMC5032244/.
853 Hayden BY, Heilbronner SR, Pearson JM, Platt ML (2011): Surprise Signals in Anterior
854 Cingulate Cortex: Neuronal Encoding of Unsigned Reward Prediction Errors Driving
855 Adjustment in Behavior. J Neurosci 31:4178–4187.
856 Hester R, Barre N, Murphy K, Silk TJ, Mattingley JB (2008): Human Medial Frontal Cortex
857 Activity Predicts Learning from Errors. Cereb Cortex 18:1933–1940.
858 Hester R, Murphy K, Brown FL, Skilleter AJ (2010): Punishing an Error Improves Learning: The
859 Influence of Punishment Magnitude on Error-Related Neural Activity and Subsequent
860 Learning. J Neurosci 30:15600–15607.
861 Huettel SA, Stowe CJ, Gordon EM, Warner BT, Platt ML (2006): Neural signatures of
862 economic preferences for risk and ambiguity. Neuron 49:765–775.
863 Ide JS, Shenoy P, Yu AJ, Li CR (2013): Bayesian Prediction and Evaluation in the Anterior
864 Cingulate Cortex. J Neurosci 33:2039–2047.
865 Iglesias S, Mathys C, Brodersen KH, Kasper L, Piccirelli M, den Ouden HEM, Stephan KE
866 (2013): Hierarchical Prediction Errors in Midbrain and Basal Forebrain during Sensory
867 Learning. Neuron 80:519–530.

868 Ikemoto S (2007): Dopamine reward circuitry: Two projection systems from the ventral
869 midbrain to the nucleus accumbens–olfactory tubercle complex. Brain Res Rev
870 56:27–78.
871 Jenkinson M, Bannister P, Brady M, Smith S (2002): Improved optimization for the robust
872 and accurate linear registration and motion correction of brain images. NeuroImage
873 17:825–841.
874 Jensen J, Smith AJ, Willeit M, Crawley AP, Mikulis DJ, Vitcu I, Kapur S (2007): Separate brain
875 regions code for salience vs. valence during reward prediction in humans. Hum Brain
876 Mapp 28:294–302.
877 Jocham G, Brodersen KH, Constantinescu AO, Kahn MC, Ianni AM, Walton ME, Rushworth
878 MFS, Behrens TEJ (2016): Reward-Guided Learning with and without Causal
879 Attribution. Neuron 90:177–190.
880 Kaelbling LP, Littman ML, Moore AW (1996): Reinforcement Learning: A Survey.
881 arXiv:cs/9605103. http://arxiv.org/abs/cs/9605103.
882 Kahnt T (2017): A decade of decoding reward-related fMRI signals and where we go from
883 here. NeuroImage.
884 http://www.sciencedirect.com/science/article/pii/S1053811917304688.
885 Kahnt T, Heinzle J, Park SQ, Haynes J-D (2010): The neural code of reward anticipation in
886 human orbitofrontal cortex. Proc Natl Acad Sci 107:6010–6015.
887 Kahnt T, Tobler PN (2013): Salience Signals in the Right Temporoparietal Junction Facilitate
888 Value-Based Decisions. J Neurosci 33:863–869.
889 Katahira K, Matsuda Y-T, Fujimura T, Ueno K, Asamizuya T, Suzuki C, Cheng K, Okanoya K,
890 Okada M (2015): Neural basis of decision making guided by emotional outcomes. J
891 Neurophysiol 113:3056–3068.
892 Klein-Flügge MC, Hunt LT, Bach DR, Dolan RJ, Behrens TEJ (2011): Dissociable reward and
893 timing signals in human midbrain and ventral striatum. Neuron 72:654–664.
894 Knutson B, Adams CM, Fong GW, Hommer D (2001): Anticipation of increasing monetary
895 reward selectively recruits nucleus accumbens. J Neurosci Off J Soc Neurosci
896 21:RC159.
897 Knutson B, Westdorp A, Kaiser E, Hommer D (2000): FMRI visualization of brain activity
898 during a monetary incentive delay task. NeuroImage 12:20–27.
899 Koch K, Schachtzabel C, Wagner G, Reichenbach JR, Sauer H, Schlösser R (2008): The neural
900 correlates of reward-related trial-and-error learning: An fMRI study with a
901 probabilistic learning task. Learn Mem 15:728–732.
902 Kolling N, Behrens TEJ, Mars RB, Rushworth MFS (2012): Neural Mechanisms of Foraging.
903 Science 336:95–98.
904 Kotz SA, Dengler R, Wittfoth M (2015): Valence-specific conflict moderation in the dorso-
905 medial PFC and the caudate head in emotional speech. Soc Cogn Affect Neurosci
906 10:165–171.
907 Kurniawan IT, Guitart-Masip M, Dayan P, Dolan RJ (2013): Effort and valuation in the brain:
908 the effects of anticipation and execution. J Neurosci Off J Soc Neurosci 33:6160–
909 6169.
910 Laird AR, Fox PM, Price CJ, Glahn DC, Uecker AM, Lancaster JL, Turkeltaub PE, Kochunov P,
911 Fox PT (2005): ALE meta-analysis: controlling the false discovery rate and performing
912 statistical contrasts. Hum Brain Mapp 25:155–164.
913 Lebreton M, Abitbol R, Daunizeau J, Pessiglione M (2015): Automatic integration of
914 confidence in the brain valuation signal. Nat Neurosci 18:1159–1167.

915 Leknes S, Lee M, Berna C, Andersson J, Tracey I (2011): Relief as a Reward: Hedonic and
916 Neural Responses to Safety from Pain. PLOS ONE 6:e17870.
917 Leong YC, Radulescu A, Daniel R, DeWoskin V, Niv Y (2017): Dynamic Interaction between
918 Reinforcement Learning and Attention in Multidimensional Environments. Neuron
919 93:451–463.
920 Li J, Daw ND (2011): Signals in human striatum are appropriate for policy update rather than
921 value prediction. J Neurosci Off J Soc Neurosci 31:5504–5511.
922 Li J, Zhang Y (2006): Prediction error method-based second-order structural identification
923 algorithm in stochastic state space formulation. Earthq Eng Struct Dyn 35:761–779.
924 Lin A, Adolphs R, Rangel A (2012): Social and monetary reward learning engage overlapping
925 neural substrates. Soc Cogn Affect Neurosci 7:274–281.
926 Litt A, Plassmann H, Shiv B, Rangel A (2011): Dissociating valuation and saliency signals
927 during decision-making. Cereb Cortex N Y N 1991 21:95–102.
928 Liu X, Hairston J, Schrier M, Fan J (2011): Common and distinct networks underlying reward
929 valence and processing stages: a meta-analysis of functional neuroimaging studies.
930 Neurosci Biobehav Rev 35:1219–1236.
931 Losecaat Vermeer A, Boksem M, G Sanfey A (2014): Neural mechanisms underlying context-
932 dependent shifts in risk preferences. NeuroImage 103.
933 Luking KR, Luby JL, Barch DM (2014): Kids, candy, brain and behavior: Age differences in
934 responses to candy gains and losses. Dev Cogn Neurosci 9:82–92.
935 Manza P, Hu S, Ide JS, Farr OM, Zhang S, Leung H-C, Li CR (2016): The effects of
936 methylphenidate on cerebral responses to conflict anticipation and unsigned
937 prediction error in a stop-signal task. J Psychopharmacol Oxf Engl 30:283–293.
938 Marsh R, Hao X, Xu D, Wang Z, Duan Y, Liu J, Kangarlu A, Martinez D, Garcia F, Tau GZ, Yu S,
939 Packard MG, Peterson BS (2010): A virtual reality-based FMRI study of reward-based
940 spatial learning. Neuropsychologia 48:2912–2921.
941 Mathys CD, Lomakina EI, Daunizeau J, Iglesias S, Brodersen KH, Friston KJ, Stephan KE
942 (2014): Uncertainty in perception and the Hierarchical Gaussian Filter. Front Hum
943 Neurosci 8. http://journal.frontiersin.org/article/10.3389/fnhum.2014.00825/full.
944 Matsumoto M, Hikosaka O (2009): Two types of dopamine neuron distinctly convey positive
945 and negative motivational signals. Nature 459:837–841.
946 Mattfeld AT, Gluck MA, Stark CEL (2011): Functional specialization within the striatum along
947 both the dorsal/ventral and anterior/posterior axes during associative learning via
948 reward and punishment. Learn Mem Cold Spring Harb N 18:703–711.
949 Maunsell JHR (2004): Neuronal representations of cognitive state: reward or attention?
950 Trends Cogn Sci 8:261–265.
951 McClure SM, Berns GS, Montague PR (2003): Temporal prediction errors in a passive
952 learning task activate human striatum. Neuron 38:339–346.
953 Menon V, Levitin DJ (2005): The rewards of music listening: response and physiological
954 connectivity of the mesolimbic system. NeuroImage 28:175–184.
955 Metereau E, Dreher J-C (2013): Cerebral correlates of salient prediction error for different
956 rewards and punishments. Cereb Cortex N Y N 1991 23:477–487.
957 Metereau E, Dreher J-C (2015): The medial orbitofrontal cortex encodes a general unsigned
958 value signal during anticipation of both appetitive and aversive events. Cortex J
959 Devoted Study Nerv Syst Behav 63:42–54.
960 Meyniel F, Dehaene S (2017): Brain networks for confidence weighting and hierarchical
961 inference during probabilistic learning. Proc Natl Acad Sci 114:E3859–E3868.

962 Middlebrooks PG, Sommer MA (2012): Neuronal correlates of metacognition in primate
963 frontal cortex. Neuron 75:517–530.
964 Montague PR, Dayan P, Sejnowski TJ (1996): A framework for mesencephalic dopamine
965 systems based on predictive Hebbian learning. J Neurosci Off J Soc Neurosci
966 16:1936–1947.
967 Morrens J (2014): Dopamine neurons coding prediction errors in reward space, but not in
968 aversive space: a matter of location? J Neurophysiol 112:1021–1024.
969 Nassar MR, Rumsey KM, Wilson RC, Parikh K, Heasly B, Gold JI (2012): Rational regulation of
970 learning dynamics by pupil-linked arousal systems. Nat Neurosci 15:1040–1046.
971 Nieuwenhuis S, Slagter HA, von Geusau NJA, Heslenfeld DJ, Holroyd CB (2005): Knowing
972 good from bad: differential activation of human cortical areas by positive and
973 negative outcomes. Eur J Neurosci 21:3161–3168.
974 Niv Y, Daniel R, Geana A, Gershman SJ, Leong YC, Radulescu A, Wilson RC (2015):
975 Reinforcement Learning in Multidimensional Environments Relies on Attention
976 Mechanisms. J Neurosci 35:8145–8157.
977 Noonan MP, Mars RB, Rushworth MFS (2011): Distinct roles of three frontal cortical areas in
978 reward-guided behavior. J Neurosci Off J Soc Neurosci 31:14399–14412.
979 O'Doherty J, Kringelbach ML, Rolls ET, Hornak J, Andrews C (2001): Abstract reward and
980 punishment representations in the human orbitofrontal cortex. Nat Neurosci 4:95–
981 102.
982 O'Doherty J, Critchley H, Deichmann R, Dolan RJ (2003): Dissociating valence of outcome
983 from behavioral control in human orbital and ventral prefrontal cortices. J Neurosci
984 Off J Soc Neurosci 23:7931–7939.
985 O'Doherty J, Dayan P, Schultz J, Deichmann R, Friston K, Dolan RJ (2004): Dissociable Roles
986 of Ventral and Dorsal Striatum in Instrumental Conditioning. Science 304:452–454.
987 O'doherty JP, Hampton A, Kim H (2007): Model-Based fMRI and Its Application to Reward
988 Learning and Decision Making. Ann N Y Acad Sci 1104:35–53.
989 Oostenveld R, Fries P, Maris E, Schoffelen J-M (2011): FieldTrip: Open Source Software for
990 Advanced Analysis of MEG, EEG, and Invasive Electrophysiological Data. Research
991 article. Computational Intelligence and Neuroscience.
992 https://www.hindawi.com/journals/cin/2011/156869/.
993 O'Reilly JX, Schüffelgen U, Cuell SF, Behrens TEJ, Mars RB, Rushworth MFS (2013):
994 Dissociable effects of surprise and model update in parietal and anterior cingulate
995 cortex. Proc Natl Acad Sci 110:E3660–E3669.
996 den Ouden HEM, Kok P, de Lange FP (2012): How Prediction Errors Shape Perception,
997 Attention, and Motivation. Front Psychol 3.
998 http://www.ncbi.nlm.nih.gov/pmc/articles/PMC3518876/.
999 Pagnoni G, Zink CF, Montague PR, Berns GS (2002): Activity in human ventral striatum
1000 locked to errors of reward prediction. Nat Neurosci 5:97–98.
1001 Paschke LM, Walter H, Steimke R, Ludwig VU, Gaschler R, Schubert T, Stelzel C (2015):
1002 Motivation by potential gains and losses affects control processes via different
1003 mechanisms in the attentional network. NeuroImage 111:549–561.
1004 Pearce JM, Hall G (1980): A model for Pavlovian learning: Variations in the effectiveness of
1005 conditioned but not of unconditioned stimuli. Psychol Rev 87:532–552.
1006 Pessiglione M, Petrovic P, Daunizeau J, Palminteri S, Dolan RJ, Frith CD (2008): Subliminal
1007 instrumental conditioning demonstrated in the human brain. Neuron 59:561–567.

Pessiglione M, Seymour B, Flandin G, Dolan RJ, Frith CD (2006): Dopamine-dependent prediction errors underpin reward-seeking behaviour in humans. Nature 442:1042–1045.
Philiastides MG, Biele G, Heekeren HR (2010a): A mechanistic account of value computation in the human brain. Proc Natl Acad Sci U S A 107:9430–9435.
Philiastides MG, Biele G, Vavatzanidis N, Kazzer P, Heekeren HR (2010b): Temporal dynamics of prediction error processing during reward-based decision making. NeuroImage 53:221–232.
Philiastides MG, Heekeren HR, Sajda P (2014): Human Scalp Potentials Reflect a Mixture of Decision-Related Signals during Perceptual Choices. J Neurosci 34:16877–16889.
Pisauro A, Fouragnan E, Retzler C, Philiastides M (2017): Neural correlates of evidence accumulation during value-based decisions revealed via simultaneous EEG-fMRI. Nat Commun. http://eprints.hud.ac.uk/31834/.
Poudel GR, Innes CRH, Jones RD (2013): Distinct neural correlates of time-on-task and transient errors during a visuomotor tracking task after sleep restriction. NeuroImage 77:105–113.
Preuschoff K, Quartz SR, Bossaerts P (2008): Human Insula Activation Reflects Risk Prediction Errors As Well As Risk. J Neurosci 28:2745–2752.
Queirazza F, Fouragnan E, Steele JD, Cavanagh J, Philiastides M (2017): Dorsomedial prefrontal cortex activity during reinforcement learning discriminates response to Cognitive Behavioural Therapy in depression. bioRxiv:224410.
R Garrison J, Done J, S Simons J (2017): Interpretation of published meta-analytical studies affected by implementation errors in the GingerALE software.
Rescorla R, Wagner A (1972): A theory of Pavlovian conditioning: Variations in the effectiveness of reinforcement and nonreinforcement. In: Black, A, Prokasy, W, editors. Classical Conditioning II: Current Research and Theory. Appleton-Century-Crofts. pp 64–99.
Ribas-Fernandes JJF, Solway A, Diuk C, McGuire JT, Barto AG, Niv Y, Botvinick MM (2011): A neural signature of hierarchical reinforcement learning. Neuron 71:370–379.
Rodriguez PF (2009): Stimulus-outcome learnability differentially activates anterior cingulate and hippocampus at feedback processing. Learn Mem Cold Spring Harb N 16:324–331.
Roesch MR, Olson CR (2004): Neuronal Activity Related to Reward Value and Motivation in Primate Frontal Cortex. Science 304:307–310.
Rohe T, Noppeney U (2015): Cortical Hierarchies Perform Bayesian Causal Inference in Multisensory Perception. PLOS Biol 13:e1002073.
Rohe T, Weber B, Fliessbach K (2012): Dissociation of BOLD responses to reward prediction errors and reward receipt by a model comparison. Eur J Neurosci 36:2376–2382.
Rolls ET, Grabenhorst F, Parris BA (2008): Warm pleasant feelings in the brain. NeuroImage 41:1504–1513.
Rudorf S, Preuschoff K, Weber B (2012): Neural Correlates of Anticipation Risk Reflect Risk Preferences. J Neurosci 32:16683–16692.
Samson RD, Frank MJ, Fellous J-M (2010): Computational models of reinforcement learning: the role of dopamine as a reward signal. Cogn Neurodyn 4:91–105.
Sarinopoulos I, Grupe DW, Mackiewicz KL, Herrington JD, Lor M, Steege EE, Nitschke JB (2010): Uncertainty during anticipation modulates neural responses to aversion in human insula and amygdala. Cereb Cortex N Y N 1991 20:929–940.

Schlagenhauf F, Rapp MA, Huys QJM, Beck A, Wüstenberg T, Deserno L, Buchholz H-G, Kalbitzer J, Buchert R, Bauer M, Kienast T, Cumming P, Plotkin M, Kumakura Y, Grace AA, Dolan RJ, Heinz A (2013): Ventral striatal prediction error signaling is associated with dopamine synthesis capacity and fluid intelligence. Hum Brain Mapp 34:1490–1499.

Scholl J, Kolling N, Nelissen N, Wittmann MK, Harmer CJ, Rushworth MFS (2015): The Good, the Bad, and the Irrelevant: Neural Mechanisms of Learning Real and Hypothetical Rewards and Effort. J Neurosci Off J Soc Neurosci 35:11233–11251.

Schonberg T, O'Doherty JP, Joel D, Inzelberg R, Segev Y, Daw ND (2010): Selective impairment of prediction error signaling in human dorsolateral but not ventral striatum in Parkinson's disease patients: evidence from a model-based fMRI study. NeuroImage 49:772–781.

Schultz W, Apicella P, Ljungberg T (1993): Responses of monkey dopamine neurons to reward and conditioned stimuli during successive steps of learning a delayed response task. J Neurosci Off J Soc Neurosci 13:900–913.

Schultz W, Apicella P, Scarnati E, Ljungberg T (1992): Neuronal activity in monkey ventral striatum related to the expectation of reward. J Neurosci Off J Soc Neurosci 12:4595–4610.

Schultz W (1998): Predictive Reward Signal of Dopamine Neurons. J Neurophysiol 80:1–27.

Schultz W (2016a): Dopamine reward prediction-error signalling: a two-component response. Nat Rev Neurosci 17:183–195.

Schultz W (2016b): Dopamine reward prediction error coding. Dialogues Clin Neurosci 18:23–32.

Schultz W, Dayan P, Montague PR (1997): A Neural Substrate of Prediction and Reward. Science 275:1593–1599.

Schwartenbeck P, FitzGerald THB, Dolan R (2016): Neural signals encoding shifts in beliefs. NeuroImage 125:578–586.

Scimeca JM, Katzman PL, Badre D (2016): Striatal prediction errors support dynamic control of declarative memory decisions. Nat Commun 7:ncomms13061.

Serences JT (2008): Value-based modulations in human visual cortex. Neuron 60:1169–1181.

Sescousse G, Caldú X, Segura B, Dreher J-C (2013): Processing of primary and secondary rewards: A quantitative meta-analysis and review of human functional neuroimaging studies. Neurosci Biobehav Rev 37:681–696.

Seymour B, Daw N, Dayan P, Singer T, Dolan R (2007): Differential Encoding of Losses and Gains in the Human Striatum. J Neurosci Off J Soc Neurosci 27:4826–4831.

Silvetti M, Verguts T (2012): Reinforcement Learning, High-Level Cognition, and the Human Brain. http://www.intechopen.com/books/neuroimaging-cognitive-and-clinical-neuroscience/reinforcement-learning-high-level-cognition-and-the-human-brain.

So N, Stuphorn V (2012): Supplementary Eye Field Encodes Reward Prediction Error. J Neurosci 32:2950–2963.

Späti J, Chumbley J, Brakowski J, Dörig N, Grosse Holtforth M, Seifritz E, Spinelli S (2014): Functional lateralization of the anterior insula during feedback processing. Hum Brain Mapp 35:4428–4439.

Spicer J, Galvan A, Hare TA, Voss H, Glover G, Casey B (2007): Sensitivity of the Nucleus Accumbens to Violations in Expectation of Reward. NeuroImage 34:455–461.

Spoormaker VI, Andrade KC, Schröter MS, Sturm A, Goya-Maldonado R, Sämann PG, Czisch M (2011): The neural correlates of negative prediction error signaling in human fear conditioning. NeuroImage 54:2250–2256.
Sutton R (1998): Reinforcement Learning: An Introduction. Cambridge, Mass: MIT Press.
Takemura H, Samejima K, Vogels R, Sakagami M, Okuda J (2011): Stimulus-Dependent Adjustment of Reward Prediction Error in the Midbrain. PLOS ONE 6:e28337.
Tanaka SC, Doya K, Okada G, Ueda K, Okamoto Y, Yamawaki S (2004): Prediction of immediate and future rewards differentially recruits cortico-basal ganglia loops. Nat Neurosci 7:nn1279.
Tanaka SC, Samejima K, Okada G, Ueda K, Okamoto Y, Yamawaki S, Doya K (2006): Brain mechanism of reward prediction under predictable and unpredictable environmental dynamics. Neural Netw Off J Int Neural Netw Soc 19:1233–1241.
Tobia MJ, Gläscher J, Sommer T (2016): Context-specific behavioral surprise is differentially correlated with activity in anterior and posterior brain systems. Neuroreport 27:677–682.
Turkeltaub PE, Eden GF, Jones KM, Zeffiro TA (2002): Meta-analysis of the functional neuroanatomy of single-word reading: method and validation. NeuroImage 16:765–780.
Ullsperger M, Cramon DY von (2003): Error Monitoring Using External Feedback: Specific Roles of the Habenular Complex, the Reward System, and the Cingulate Motor Area Revealed by Functional Magnetic Resonance Imaging. J Neurosci 23:4308–4314.
Valentin VV, O'Doherty JP (2009): Overlapping prediction errors in dorsal striatum during instrumental learning with juice and money reward in the human brain. J Neurophysiol 102:3384–3391.
Watanabe N, Sakagami M, Haruno M (2013): Reward Prediction Error Signal Enhanced by Striatum–Amygdala Interaction Explains the Acceleration of Probabilistic Reward Learning by Emotion. J Neurosci 33:4487–4493.
Wittmann MK, Kolling N, Akaishi R, Chau BKH, Brown JW, Nelissen N, Rushworth MFS (2016): Predictive decision making driven by multiple time-linked reward representations in the anterior cingulate cortex. Nat Commun 7:12327.
Wunderlich K, Rangel A, O'Doherty JP (2009): Neural computations underlying action-based decision making in the human brain. Proc Natl Acad Sci 106:17199–17204.
Wunderlich K, Symmonds M, Bossaerts P, Dolan RJ (2011): Hedging your bets by learning reward correlations in the human brain. Neuron 71:1141–1152.
Yacubian J, Gläscher J, Schroeder K, Sommer T, Braus DF, Büchel C (2006): Dissociable systems for gain- and loss-related value predictions and errors of prediction in the human brain. J Neurosci Off J Soc Neurosci 26:9530–9537.
Yeung N, Sanfey AG (2004): Independent Coding of Reward Magnitude and Valence in the Human Brain. J Neurosci 24:6258–6264.
Yu AJ, Dayan P (2005): Uncertainty, Neuromodulation, and Attention. Neuron 46:681–692.
Zalla T, Koechlin E, Pietrini P, Basso G, Aquino P, Sirigu A, Grafman J (2000): Differential amygdala responses to winning and losing: a functional magnetic resonance imaging study in humans. Eur J Neurosci 12:1764–1770.
Zhang S, Mano H, Ganesh G, Robbins T, Seymour B (2016): Dissociable Learning Processes Underlie Human Pain Conditioning. Curr Biol 26:52–58.
Zink CF, Pagnoni G, Martin-Skurski ME, Chappelow JC, Berns GS (2004): Human striatal responses to monetary reward depend on saliency. Neuron 42:509–517.

Table 1. Categorisation of fMRI studies into the three RPE components (valence, surprise, signed RPE) and broken down by the relevant fMRI contrast/regressor.

Statistical comparisons	Number	Total	Reference
Valence ***Pattern A i (NEG>POS)***		32	[de Bruijn et al., 2009; Daniel et al., 2011; Demos et al., 2012; van Duijvenvoorde et al., 2014; Elward et al., 2015; Ferdinand and Opitz, 2014; Fouragnan et al., 2015; Gläscher et al., 2009; Haruno et al., 2004; Häusler et al., 2016; Jocham et al., 2016; Kahnt et al., 2010; Katahira et al., 2015; Klein-Flügge et al., 2011; Klein-Flügge et al., 2011; Knutson et al., 2000; Knutson et al., 2001; Koch et al., 2008; Leknes et al., 2011; Losecaat Vermeer et al., 2014; Marsh et al., 2010; Mattfeld et al., 2011; Noonan et al., 2011; O'Doherty et al., 2001; O'Doherty et al., 2003; Rodriguez, 2009; Rolls et al., 2008; Scholl et al., 2015; Seymour et al., 2007; Spicer et al., 2007; Spoormaker et al., 2011; Ullsperger and Cramon, 2003; Yacubian et al., 2006]
Negative > Positive	19		
Negative > No outcomes	9		
Negative correlation with a regressor defining valence RPE (with a binary modulation whereby positive RPE = 1, and negative RPE = -1)	4		
Valence ***Pattern A ii (POS>NEG)***		33	[Amiez et al., 2012; Aron et al., 2004; Bickel et al., 2009; de Bruijn et al., 2009; Canessa et al., 2013; Daniel et al., 2011; van Duijvenvoorde et al., 2014; Elliott et al., 2000; Ernst et al., 2004; Forster and Brown, 2011; Fouragnan et al., 2015; Fujiwara et al., 2009; Häusler et al., 2016; Hester et al., 2008; Hester et al., 2010; Jocham et al., 2016; Katahira et al., 2015; Knutson et al., 2000; Knutson et al., 2001; Knutson et al., 2001; Kurniawan et al., 2013; Losecaat Vermeer et al., 2014; Luking et al., 2014; Paschke et al., 2015; Sarinopoulos et al., 2010; Scholl et al., 2015; Schonberg et al., 2010; Seymour et al., 2007; Späti et al., 2014; Spoormaker et al., 2011; Ullsperger and Cramon, 2003]
Positive > Negative	18		
Positive > No outcomes	9		
Positive correlation with a regressor defining valence RPE (with a binary modulation whereby positive RPE = 1, and negative RPE = -1)	6		
Surprise ***Pattern B***		41	[Allen et al., 2016; Amado et al., 2016; Amiez et al., 2012; Boll et al., 2013; Browning et al., 2010; Chumbley et al., 2014; Daw et al., 2011; Dreher, 2013; Ferdinand and Opitz, 2014; Forster and Brown, 2011; Fouragnan et al., 2015; Fouragnan et al., 2017; Fujiwara et al., 2009; Ide et al., 2013; Iglesias et al., 2013; Jensen et al., 2007; Knutson et al., 2001; Kotz et al., 2015; Leong et al., 2017; Losecaat Vermeer et al., 2014; Manza et al., 2016; McClure et al., 2003; Metereau and Dreher, 2013; Metereau and Dreher, 2015; Meyniel and Dehaene, 2017; Nieuwenhuis et al., 2005; O'Reilly et al., 2013; den Ouden et al., 2012; Poudel et al., 2013; Rodriguez, 2009; Rohe et al., 2012; Rohe and Noppeney, 2015; Rohe and Noppeney, 2015; Rolls et al., 2008; Schwartenbeck et al., 2016; Silvetti and Verguts, 2012; Tobia et al., 2016; Watanabe et al., 2013; Wunderlich et al., 2009; Wunderlich et al., 2011; Yacubian et al., 2006; Zalla et al., 2000; Zhang et al., 2016]
Unsigned RPE ("RL surprise")	12		
Unsigned Bayesian RPE ("Volatility", "Bayesian surprise")	13		
Positive and Negative outcomes > No or low outcomes	9		
"Associability" term of the Pearce et Hall model	2		
Parametric changes in magnitude of surprising positive RPE (unsigned)	3		
Parametric changes in magnitude of surprising negative RPE (unsigned)	2		
Signed RPE ***Pattern C***		38	[Abler et al., 2006; Behrens et al., 2007; van den Bos et al., 2012; Cohen and Ranganath, 2007; Daw et al., 2011; Delgado et al., 2000; Delgado, 2007; Diederen et al., 2017; Diuk et al., 2013; Dunne et al., 2016; Gläscher et al., 2010; Guo et al., 2016; Hare et al., 2008; Ide et al., 2013; Katahira et al., 2015; Leong et al., 2017; Li and Zhang, 2006; Lin et al., 2012; Mattfeld et al., 2011; McClure et al., 2003; Metereau and Dreher, 2013; Metereau and Dreher, 2015; O'Doherty et al., 2003; Pessiglione et al., 2006; Pessiglione et al., 2008; Ribas-Fernandes et al., 2011; Rolls et al., 2008; Schlagenhauf et al., 2013; Schonberg et al., 2010; Scimeca et al., 2016; Seymour et al., 2007; Takemura et al., 2011; Tanaka et al., 2004; Tanaka et al., 2006; Valentin and O'Doherty, 2009; Watanabe et al., 2013; Wunderlich et al., 2011]
Signed RPE (from model-free RL models)	16		
Signed RPE (from model-based RL models)	8		
Signed Bayesian RPE	10		
High positive RPEs > low positive RPEs > low negative RPEs > high negative RPEs	4		

Table 2. ALE cluster results for the valence analysis: Pattern A (i) and (ii) (FDR-ID P < 0.05, with a minimum volume cluster size of 50 mm^3.

Region	R/L	*x*	*y*	*z*	Cluster size	ALE score
Pattern A (i) NEG > POS						
Dorsomedial cingulate cortex (dMCC)	R	2	24	36	12712	0.051
Anterior Insula (aINS)	R	32	24	-2	6120	0.062
-	L	-32	22	-4	4880	0.056
Pallidum	R	12	8	4	3360	0.04
-	L	-14	6	2	2520	0.029
Middle Frontal Gyrus	R	38	4	32	3152	0.029
-	R	30	10	56	488	0.021
-	L	-28	12	60	104	0.019
Inferior Parietal Lobule (IPL)	R	40	-48	42	2416	0.039
-	L	-38	-48	42	2216	0.043
Middle Temporal Gyrus (MTG)	R	60	-28	-6	1192	0.031
Amygdala	R	18	-6	-12	704	0.024
Thalamus	L	-12	-12	10	624	0.025
-	L	-6	-26	8	280	0.023
Habenula	R	2	-20	-18	312	0.022
Dorsolateral Prefrontal Cortex (dlPFC)	L	-44	28	32	360	0.020
-	R	40	34	30	344	0.020
Fusiform Area	L	-40	-62	-10	272	0.023
Precentral Cortex	L	-52	0	34	256	0.021
Dorsomedial Orbitofrontal Cortex (dmOFC)	R	38	58	-2	192	0.020
Dorsomedial Prefrontal Cortex (dmPFC)	R	20	50	4	120	0.018
Superior Temporal Sulcus	R	58	-42	22	120	0.017
Pattern A (ii) (POS > NEG)						
Ventral striatum (vSTR)	L	-12	8	-4	4880	0.052
-	R	8	8	-2	2880	0.038
Ventromedial Prefrontal Cortex (vmPFC)	L	-2	42	0	3416	0.037
Posterior Cingulate Cortex (PCC)	L	0	-32	36	240	0.016
-	L	0	-36	26	88	0.014
Ventrolateral OFC (vlOFC)	R	32	44	-10	144	0.015
Dorsomedial Prefrontal Cortex (dmPFC)	L	-6	-56	14	96	0.016
Medial Prefrontal Cortex (mPFC)	L	-2	46	20	88	0.014

Table 3. ALE clusters results for the surprise analysis (FDR-ID P < 0.05, with a minimum volume cluster size of 50 mm^3).

Region	R/L	*x*	*y*	*z*	Cluster size	ALE score
Anterior mid-cingulate Cortex (aMCC)	R	4	24	34	4072	0.029
Anterior Insula (aINS)	R	32	24	-4	2496	0.050
-	L	-32	20	-4	1544	0.038
Inferior Parietal Lobule (IPL)	R	40	-46	42	1672	0.033
-	L	-40	-48	42	568	0.025
Dorsal Striatum (dSTR)	R	12	8	4	1400	0.034
-	L	-14	10	2	1216	0.021
Middle Temporal Gyrus (MTG)	R	60	-28	-8	648	0.022
Lateral Inferior Frontal Cortex	R	52	10	18	488	0.025
Lateral Central Frontal Gyrus	L	-44	26	30	392	0.019
Precentral Gyrus	R	48	12	34	360	0.019
-	L	-52	0	34	224	0.020
Midbrain	R	2	-20	-18	304	0.021
Dorsal mid-cingulate cortex (dMCC)	R	12	14	42	224	0.019
Hippocampus	R	20	-6	-10	160	0.018
Fusiform Gyrus	L	-40	-60	-10	112	0.017
Mid Occipital Pole	L	-16	-90	-6	112	0.016
Superior Temporal Sulcus	R	60	-40	20	64	0.015

Table 4. ALE cluster results for the conjunction analysis of valence and surprise (FDR-ID p < 0.05, with a minimum volume cluster size of 50 mm^3).

Region	R/L	*x*	*y*	*z*	Cluster size	ALE score
Striatum (STR)	R	12	6	4	1082	0.031
-	L	-12	12	4	376	0.021
Anterior Insula (aINS)	L	-32	20	-6	453	0.018
Anterior Mid-cingulate cortex (aMCC)	R	3	22	37	221	0.014
Inferior Parietal Lobule	L	40	-46	42	327	0.014

Table 5. ALE cluster results for the contrast analyses of valence and surprise (FDR-pN p < 0.05, with a minimum volume cluster size of 50 mm^3).

Region	R/L	*x*	*y*	*z*	Cluster size	ALE score
Valence vs. Surprise						
Ventral Striatum (vSTR)	L	-10	8	-10	1096	3.29
ventromedial prefrontal cortex (vmPFC)	L	-2	44	0	256	3.29
Positive vs. Surprise						
Ventral Striatum (vSTR)	L	-12	-8	-8	1872	3.29
ventromedial prefrontal cortex (vmPFC)	R	0	46	0	512	3.29
Ventral Striatum (vSTR)	R	8	8	-6	168	3.29
Negative vs. Surprise						
Middle Insula (mINS)	R	40	10	2	544	3.29
Mid Cingulate Cortex (MCC)	R	6	20	42	144	3.29
Surprise vs. Valence						
Anterior Insula (aINS)	R	32	24	-4	1224	3.29
Anterior Insula (aINS)	L	-32	20	-2	112	3.29
Ventral Tegmental Area (VTA)	L	-6	-16	-10	96	3.29
Ventral Tegmental Area (VTA)	R	2	-20	-16	72	3.29
Occipital Lobe	R	24	-80	-6	72	3.29
Surprise vs. Positive						
Anterior Insula (aINS)	R	32	22	-2	1648	3.29
Middle Temporal Gyrus (MTG)	R	40	-46	42	1184	3.29
Anterior Insula (aINS)	L	-32	22	-2	1016	3.29
Inferior Frontal Gyrus	R	52	10	18	184	3.29
Supplementary Motor Area (SMA)	L	-2	12	52	160	3.29
Surprise vs. Negative						
Angular Gyrus	R	40	-46	40	248	3.29
Anterior Insula (aINS)	R	32	28	-6	80	3.29
Dorsal Striatum (dSTR)	R	12	10	2	56	3.29

Table 6. ALE clusters results for the signed RPE studies (FDR-ID p < 0.05, with a minimum volume cluster size of 50 mm^3).

Region	R/L	*x*	*y*	*z*	Cluster size	ALE score
Striatum (STR) (encompasses left and right hemispheres)	R	12	10	-4	10888	0.053
Putamen	R	30	-6	8	688	0.024
Anterior Mid-cingulate Cortex (aMCC)	R	6	26	46	160	0.018
-	L	-2	14	40	120	0.016
Anterior Cingulate Cortex (ACC)	R	4	36	20	112	0.017
Ventromedial prefrontal (vmPFC)	L	0	34	0	64	0.015
Lateral Inferior Frontal Gyrus (lIFC)	L	-46	4	24	64	0.016

Table 7. ALE cluster results for the contrast analyses of signed RPE and valence as well as signed RPE and surprise (FDR-pN p < 0.05, with a minimum volume cluster size of 50 mm^3).

Region	R/L	*x*	*y*	*z*	Cluster size	ALE score
Positive – Signed RPE						
Ventromedial Prefrontal Cortex (vmPFC)	R	2	44	-15	160	3.29
Signed RPE - Positive						
No significant						
Negative – Signed RPE						
Middle Insula (mINS)	R	40	12	0	528	3.29
Dorsal Middle Cingulate Cortex (dMCC)	R	6	22	36	208	3.29
Middle Insula (mINS)	L	-38	18	-4	184	3.29
Habenula	L	-2	-26	8	168	2.58
Thalamus	R	8	-10	5	96	2.58
Signed RPE - Negative						
Ventral Striatum (vSTR)	R	10	10	-6	2208	3.29
Valence – Signed RPE						
Ventromedial Prefrontal Cortex (vmPFC)	R	2	44	-12	760	3.29
Middle Insula (mINS)	R	40	12	2	568	2.58
Dorsal Middle Cingulate Cortex (dMCC)	R	6	24	38	480	2.58
Signed RPE - Valence						
Ventral Striatum (vSTR)	R	12	16	-2	184	3.29
Surprise – Signed RPE						
Anterior Insula (aINS)	L	-34	22	0	704	3.29
Anterior Midcingulate Cortex (aMCC)	R	0	14	52	136	3.29
Pre supplementary motor area (preSMA)	R	0	14	52	136	3.29
Anterior Insula (aINS)	R	38	18	-2	88	3.29

Signed RPE - Surprise						
Ventral Striatum (vSTR)	L	-10	8	-10	904	3.29
Ventral Striatum (vSTR)	R	12	14	-3	192	3.29
Ventral Striatum (vSTR)	R	4	6	-6	72	3.29

1172

Figure Legends

Figure 1. Hypothesized profiles for BOLD responses as function of the three RPE components. Pattern A (i and ii) describe the two categorical valence responses (orange and blue colours indicate (i) responses being greater for negative compared to positive outcomes [NEG > POS] and (ii) responses being greater for positive compared to negative outcomes [POS > NEG]). Pattern B captures surprise effects with greater responses to higher outcome deviations from expectations, independent of the sign (valence) of the RPE. Pattern C shows a monotonically increasing response profile consistent with a signed RPE representation.

Figure 2. Results of whole-brain ALE analysis along the valence component. Overlays of brain areas activated by correlations with NEG > POS (blue) and POS > NEG (orange) (Pattern A (i) and (ii), respectively; Fig. 1) (P-values corrected with FDR-ID [FID] and FDR-pN [FRN] < 0.05 and a minimum cluster volume of 50 mm^3). Representative slices are shown with MNI coordinates given below each image.

Figure 3. Results of the whole brain ALE analysis for the surprise component of RPE (pattern B, Figure 1). Overlay of brain areas activated by all analyses representing direct or indirect measures of the surprise component of RPE (P-values corrected with FDR-ID [FID] and FDR-pN [FRN] < 0.05 and a minimum cluster volume of 50 mm^3). Representative slices are shown with MNI coordinates given below each image.

Figure 4. Results of the ALE conjunction analysis between valence and surprise (purple). The regions identified earlier with separate ALE analyses along the valence (NEG > POS: blue, POS > NEG: orange) and surprise (green) components are shown for comparison purposes. P-values were corrected with FDR-pN [FRN] < 0.05 and a minimum cluster volume of 50 mm^3 for the initial maps. Representative slices are shown with MNI coordinates given bellow each image.

Figure 5. Results of the ALE contrast analyses for [valence – surprise] (left panel) and [surprise – valence]. P-values were corrected with FDR-pN [FRN] < 0.05 and a minimum cluster volume of 50 mm^3 for the initial maps. Representative slices are shown with MNI coordinates given bellow each image.

Figure 6. Results of whole brain ALE analysis for signed RPE. Overlay of brain areas activated by positive correlation with signed RPE (P-values corrected with FDR-ID [FID] and FDR-pN [FRN] < 0.05 and a minimum cluster volume of 50 mm^3). Representative slices are shown with MNI coordinates given bellow each image.

Figure 7. Results of the ALE conjunction analysis for all components of RPE. Overlay of brain areas individually activated by (1) valence (orange), (2) surprise (green), and (3) signed RPE (red), with P-values corrected with FDR-pN [FRN] < 0.05 and a minimum cluster volume of 50 mm^3 for the initial maps. Importantly, the overlap between the three analyses, shown in white, also corresponds to the only cluster found for the ALE conjunction analysis between valence/surprise vs. signed RPE. MNI coordinates are given below each image.

Figure 8. Results of the ALE contrast analyses for [signed RPE – positive valence] (left panel), [signed RPE – negative valence] (middle panel) and [signed RPE – (positive + negative valence)] (right panel). P-values were corrected with FDR-pN [FRN] < 0.05 and a minimum cluster volume of 50 mm^3 for the initial maps. Representative slices are shown with MNI coordinates given bellow each image.

1224 Fig. 1

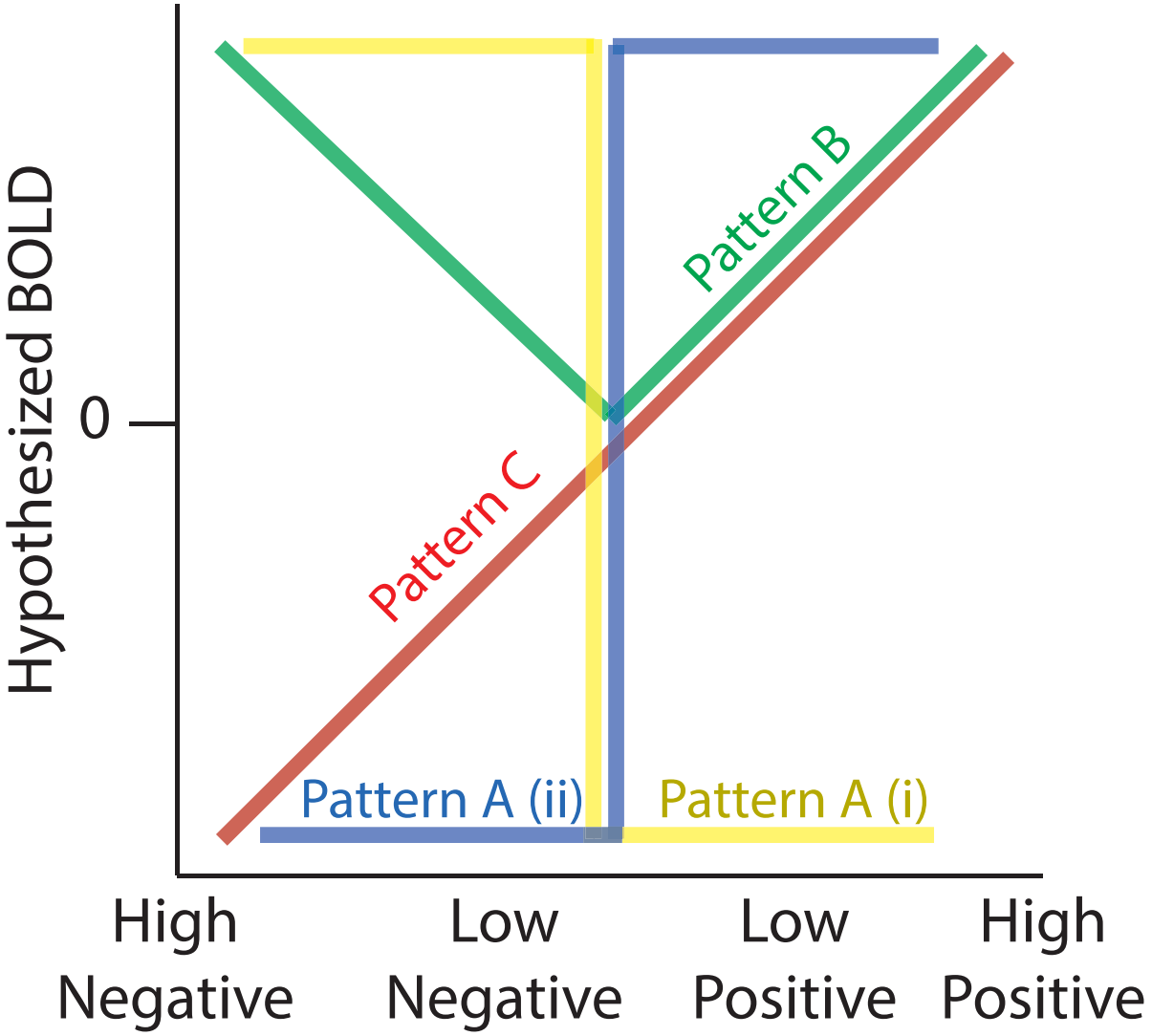

1225
1226

1227 Fig. 2

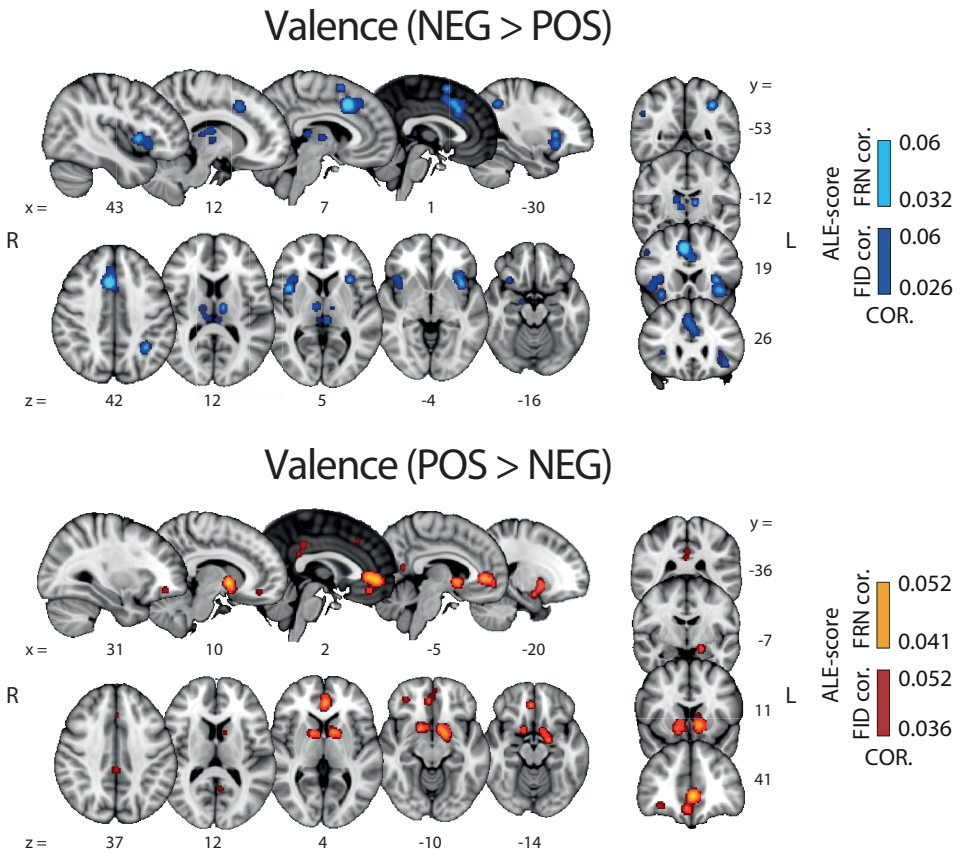

1228

1229 Fig. 3

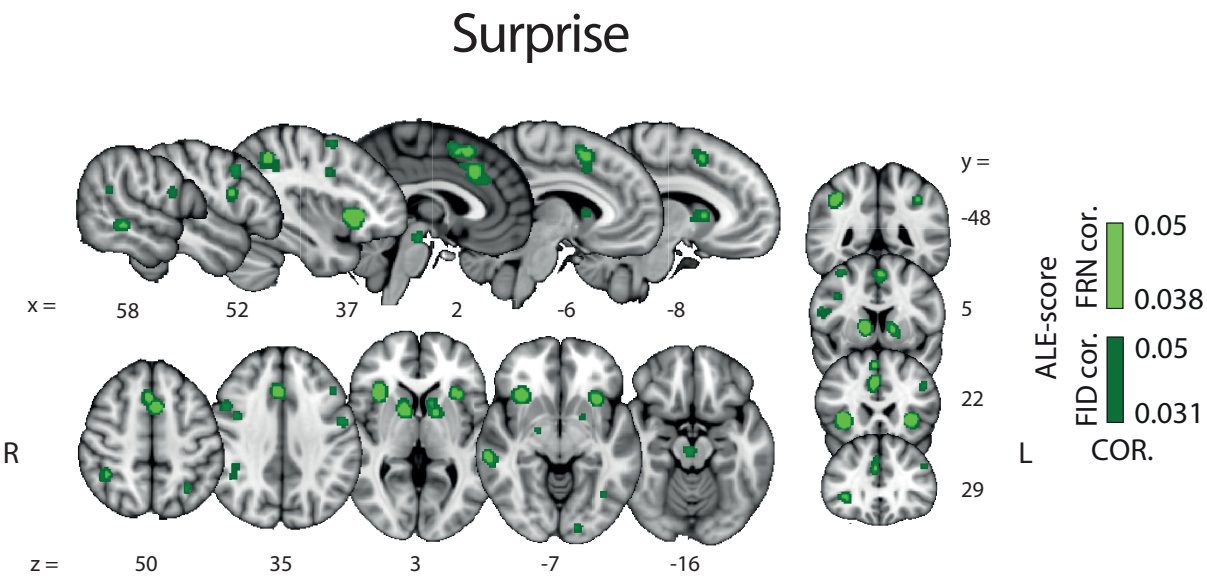

1230

1231 Fig. 4

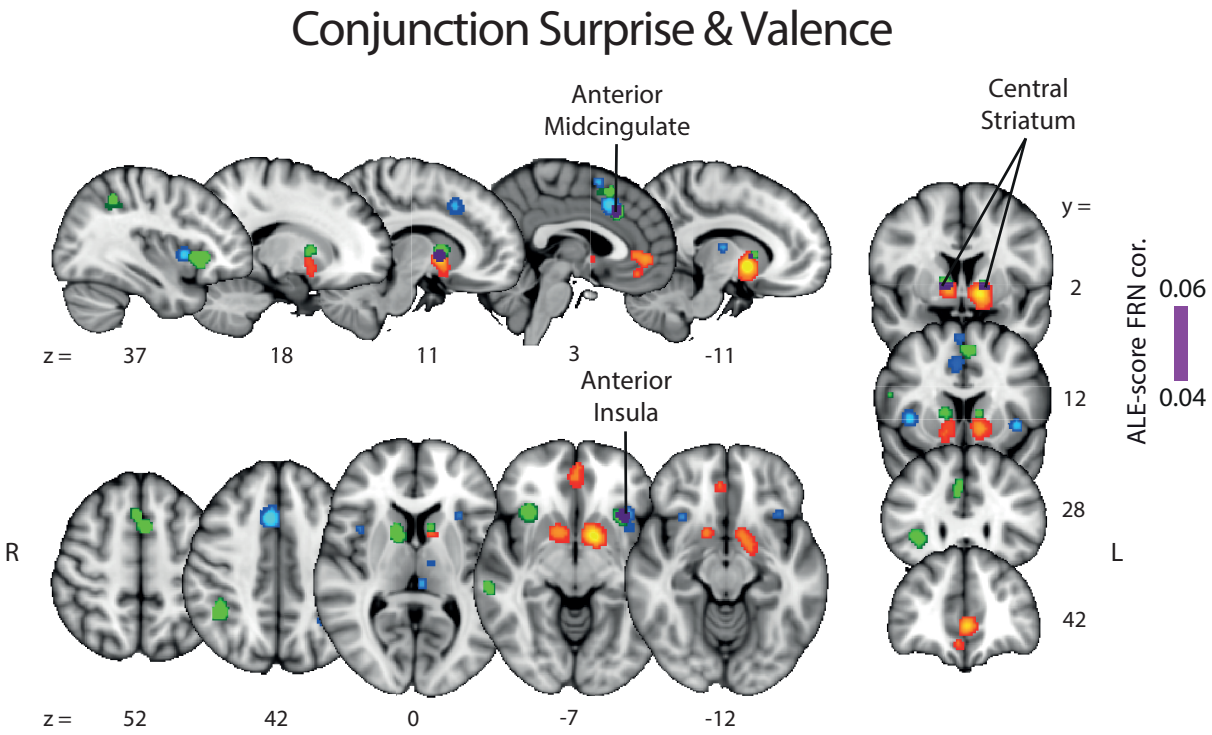

1232

Fig. 5

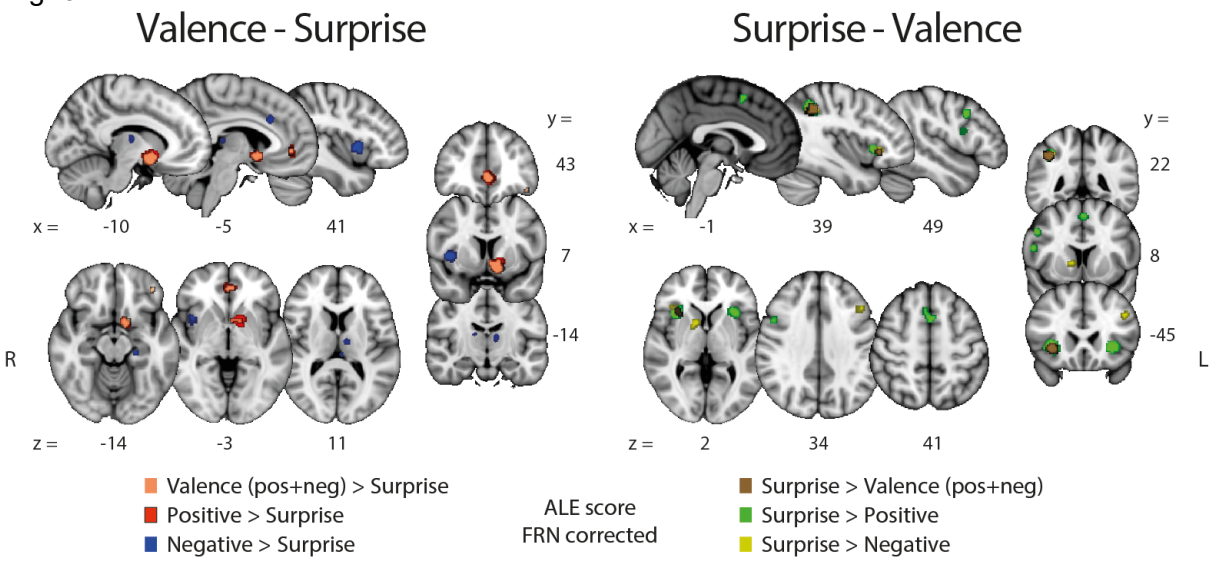
Valence - Surprise
Surprise - Valence
x = -10 -5 41
y = 43 7 -14
z = -14 -3 11
R
x = -1 39 49
y = 22 8 -45
z = 2 34 41
L
Valence (pos+neg) > Surprise
Positive > Surprise
Negative > Surprise
ALE score
FRN corrected
Surprise > Valence (pos+neg)
Surprise > Positive
Surprise > Negative

1236 Fig. 6

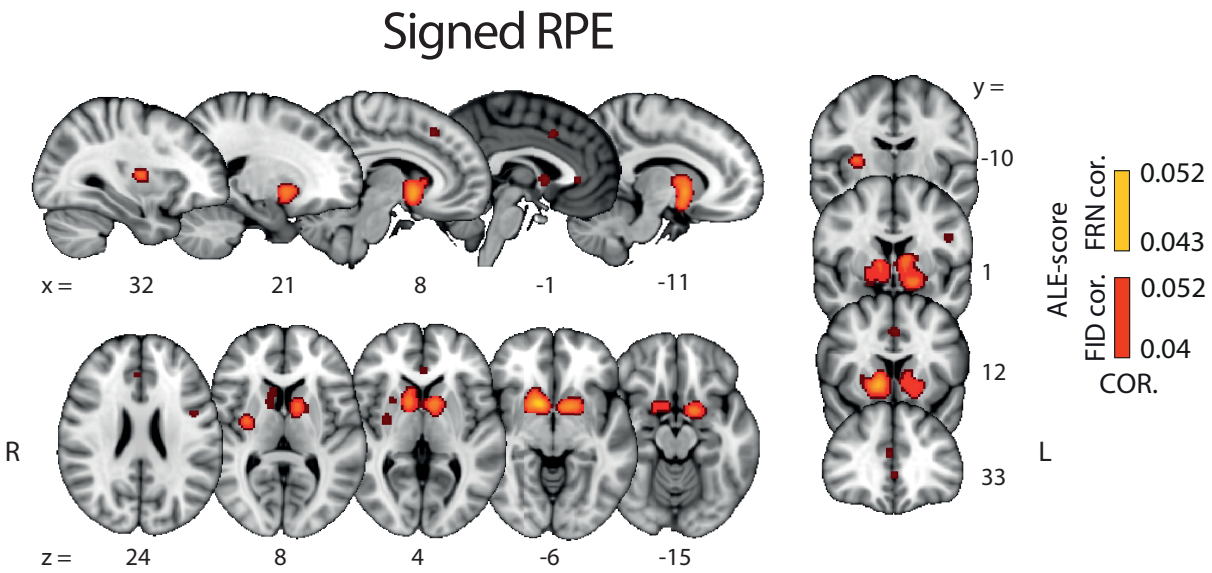

1237

1238 Fig. 7

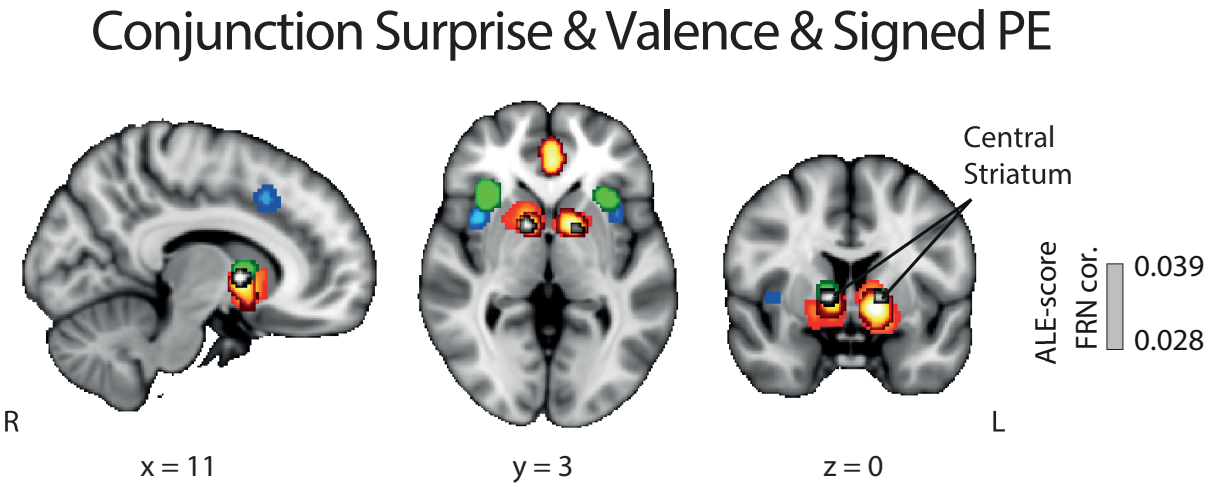

1239

1240 Fig. 8

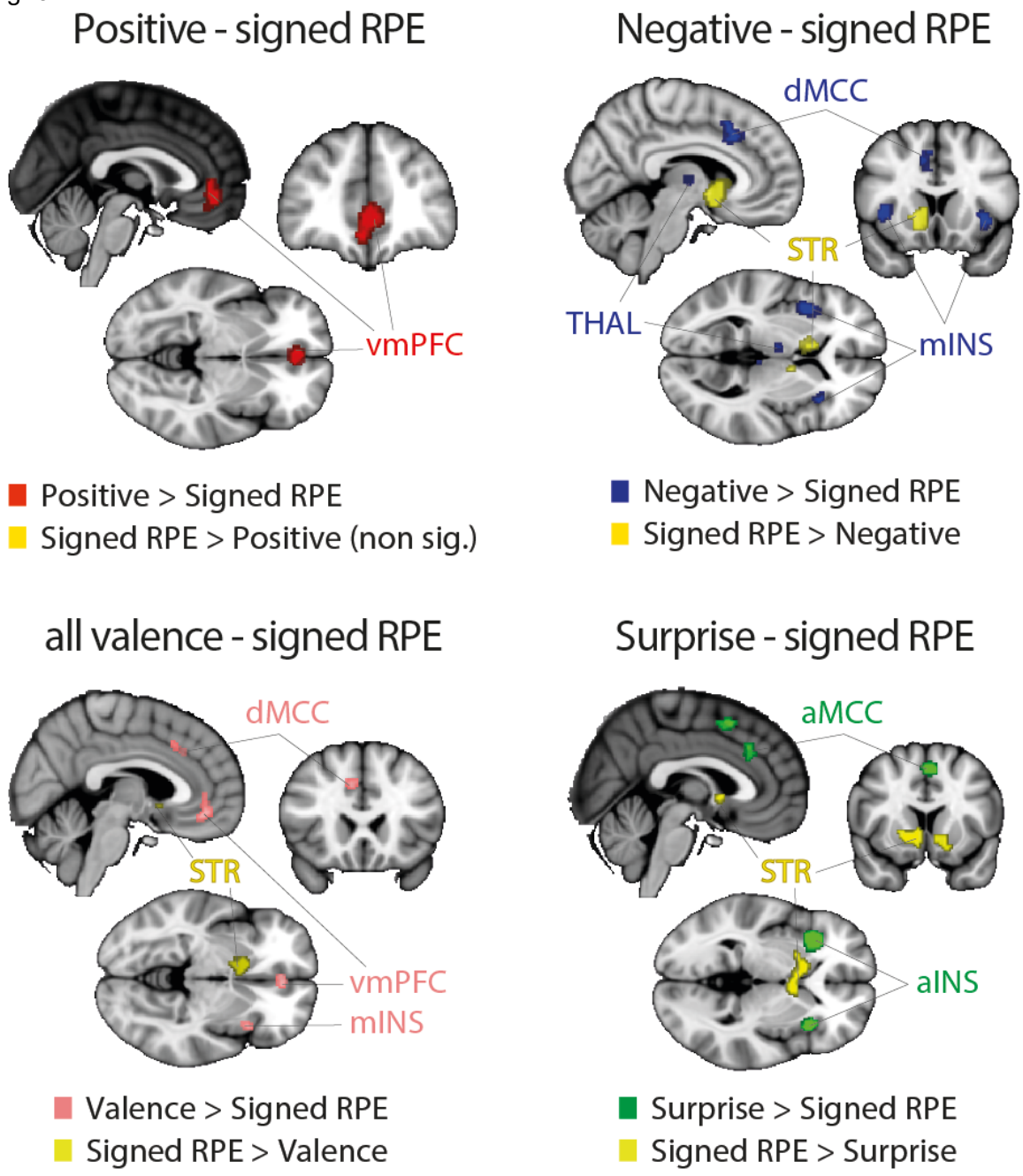

1241